

AD-A248 487



WL-TR-91-3064

INFLUENCE OF STRUCTURAL AND AERODYNAMIC MODELING ON  
FLUTTER ANALYSIS AND STRUCTURAL OPTIMIZATION

Dr. Alfred G. Striz  
The University of Oklahoma  
School of Aerospace and Mechanical Engr.  
865 Asp Avenue, Room 212  
Norman, OK 73019-0601

June 1991

DTIC  
ELECTE  
APR 07 1992  
S D D

Interim Report for Period June 90 - Dec 90

Approved for public release; distribution unlimited

FLIGHT DYNAMICS DIRECTORATE  
WRIGHT LABORATORY  
AIR FORCE SYSTEMS COMMAND  
WRIGHT-PATTERSON AIR FORCE BASE, OHIO 45433-6553

92 4 06 171

92-08890




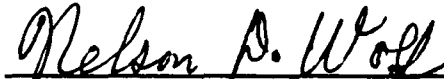
## NOTICE

When Government drawings, specifications, or other data are used for any purpose other than in connection with a definitely Government-related procurement, the United States Government incurs no responsibility or any obligation whatsoever. The fact that the government may have formulated or in any way supplied the said drawings, specifications, or other data, is not to be regarded by implication, or otherwise in any manner construed, as licensing the holder, or any other person or corporation; or as conveying any rights or permission to manufacture, use, or sell any patented invention that may in any way be related thereto.


This report is releasable to the National Technical Information Service (NTIS). At NTIS, it will be available to the general public, including foreign nations.

This technical report has been revised and is approved for publication.

  
STEPHEN M. RASMUSSEN, Capt, USAF  
Project Engineer  
Design & Analysis Methods Group

  
NELSON D. WOLF  
Technical Manager  
Design & Analysis Methods Group  
Analysis & Optimization Branch

FOR THE COMMANDER

  
DAVID K. MILLER, Lt Col, USAF  
Chief, Analysis & Optimization Branch  
Structures Division

If your address has changed, if you wish to be removed from our mailing list, or if the addressee is no longer employed by your organization please notify WL/FIBRA, WPAFB, OH 45433-6553 to help us maintain a current mailing list.

Copies of this report should not be returned unless return is required by security considerations, contractual obligations, or notice on a specific document.

REPORT DOCUMENTATION PAGE			Form Approved OMB No. 0704-0188	
Public reporting burden for this collection of information is estimated to average 1 hour per response, including the time for reviewing instructions, searching existing data sources, gathering and maintaining the data needed, and completing and reviewing the collection of information. Send comments regarding this burden estimate or any other aspect of this collection of information, including suggestions for reducing this burden, to Washington Headquarters Services, Directorate for Information Operations and Reports, 1215 Jefferson Davis Highway, Suite 1204, Arlington, VA 22202-4302, and to the Office of Management and Budget, Paperwork Reduction Project (0704-0188), Washington, DC 20503.				
1. AGENCY USE ONLY (Leave blank)		2. REPORT DATE June 30, 1991	3. REPORT TYPE AND DATES COVERED Interim Report June 1990 - Dec 1990	
4. TITLE AND SUBTITLE Influence of Structural and Aerodynamic Modeling on Flutter Analysis and Structural Optimization			5. FUNDING NUMBERS PR 2401 TA 02 WU 77 PE 62201F C F33615-87-C-3228	
6. AUTHOR(S) Striz, Alfred G.				
7. PERFORMING ORGANIZATION NAME(S) AND ADDRESS(ES) School of Aerospace and Mechanical Engineering University of Oklahoma Norman, Oklahoma 73019			8. PERFORMING ORGANIZATION REPORT NUMBER ASIAC #1090.10	
9. SPONSORING/MONITORING AGENCY NAME(S) AND ADDRESS(ES) Wright Laboratory Flight Dynamics Directorate Structures Division (WL/FIBR) Wright-Patterson AFB OH 45433-6553 D. Veley (513) 255-6992			10. SPONSORING/MONITORING AGENCY REPORT NUMBER WL-TR-91- 3064	
11. SUPPLEMENTARY NOTES Prepared in cooperation with the Aerospace Structures Information and Analysis Center.				
12a. DISTRIBUTION / AVAILABILITY STATEMENT Approved for Public Release; Distribution Unlimited.			12b. DISTRIBUTION CODE	
13. ABSTRACT (Maximum 200 words) The influences of structural and aerodynamic modeling on the flutter analysis and multidisciplinary optimization of fully built-up finite element wing models in an aeroelastic environment are not yet well understood. Therefore, the dynamic aeroelastic and optimization capabilities in the Automated STRuctural Optimization System (ASTROS) were used to evaluate the flutter behavior and the behavior of structural optimization with flutter constraints of various representative fully built-up finite element wing models in subsonic and supersonic flow. ASTROS was here used as a tool to calculate flutter speeds and frequencies and to minimize the weight of these wing models in subsonic and supersonic flow under given flutter and frequency constraints to determine the effect that these modeling factors have.				
14. SUBJECT TERMS STRUCTURES                      ASTROS AEROELASTICITY                MODELLING OPTIMIZATION			15. NUMBER OF PAGES 69	
			16. PRICE CODE	
17. SECURITY CLASSIFICATION OF REPORT UNCLASSIFIED	18. SECURITY CLASSIFICATION OF THIS PAGE UNCLASSIFIED	19. SECURITY CLASSIFICATION OF ABSTRACT UNCLASSIFIED	20. LIMITATION OF ABSTRACT UL	

## ACKNOWLEDGMENTS

This report was prepared based on research which the author performed while consulting for ASIAC, Anamet Laboratories, Inc., as a Visiting Scientist at the Wright Laboratory, WL/FIBR, Wright-Patterson Air Force Base, Ohio, from 25 May 1990 to 17 August 1990 as well as some additional work performed at the University of Oklahoma during Fall 1989, Spring 1990, and Fall 1990. Extensive scientific discussions with Dr. V.B. Venkayya, help with ASTROS from Raymond Kolonay and with NASTRAN from Victoria Tischler, both of FIBRA, and informative discussions on aeroelasticity with Dr. Frank E. Eastep of the University of Dayton and with Mark French and Dr. Max Blair of FIBRC are gratefully acknowledged. Also, Dr. James E. Marsh is commended for the efficient administration of the contract. Finally, the author would especially like to thank Dr. Venkayya for his efforts in making this second summer experience possible as well as for continuing to provide a scholarly environment highly conducive to research.

Accession For	
NTIS CRA&I	<input checked="checked" type="checkbox"/>
DTIC TAB	<input type="checkbox"/>
Unannounced	<input type="checkbox"/>
Justification	
By	
Distribution /	
Availability Codes	
Dist	Avail and/or Special
A-1	

## TABLE OF CONTENTS

Section		Page
	Acknowledgments .....	iii
	Table of Contents .....	v
	List of Figures .....	vi
	List of Tables .....	vii
I	Introduction .....	1
II	Influence of Structural and Aerodynamic Modeling on Flutter Analysis and Structural Optimization with Flutter Constraint .....	4
	1 Introduction .....	4
	2 Background .....	7
	3 The Rudisill and Bhatia Wing Model .....	10
	4 Three Wing Models with Different Aspect Ratios .....	17
	a. High Aspect Ratio Wing Model .....	19
	b. Medium Aspect Ratio Wing Model .....	25
	c. Low Aspect Ratio Wing Model .....	37
	5 Discussions and Recommendations .....	46
	References .....	50
	Appendix A: Influence of Parameter Selection on Structural Optimization with Flutter Constraint for Medium Aspect Ratio Wing Model .....	52
	1 Variation in Splining .....	52
	2 Variation in MPCs .....	54
	3 Results and Discussion .....	56
	Appendix B: Modification of Low Aspect Ratio Wing Model for Multidisciplinary Optimization .....	60
	1 Modified Low Aspect Ratio Wing Model .....	60
	2 Offset from Fuselage Center Line .....	62
	3 Aerodynamic Modeling .....	64
	Appendix C: Inclusion of Transonic Aerodynamics into the Optimization Process .....	66

## LIST OF FIGURES

Figure		Page
1	Wing Model of Reference 8 . . . . .	6
2	Wing Models Used in the Flutter Analysis and Optimization Test Cases .	8
3	High Aspect Ratio Wing Model . . . . .	22
4	V-g Plots for High Aspect Ratio Wing: a) 7 Ribs, b) 14 Ribs, c) 21 Ribs 26 Design Variables . . . . .	26
5	Medium Aspect Ratio Wing Model . . . . .	27
6	V-g Plot for Medium Aspect Ratio Wing: All MPCs, 50-Hz Upper Bound	35
7	Low Aspect Ratio Wing Model . . . . .	39
8	V-g Plots for Low Aspect Ratio Wing Model: a) 5 Spars, b) 10 Spars 15x15 Aero Mesh . . . . .	44
B-1	Modified Low Aspect Ratio Wing Model for Multidisciplinary Optimization . . . . .	61

## LIST OF TABLES

Table		Page
1	Varying Element Types on Wing Model of Reference 8 Flutter Analysis . . . . .	12
2	Varying Aerodynamic Paneling Schemes on Modified Wing Model of Reference 8 - Flutter Analysis . . . . .	14
3	Varying Element Types on Wing Model of Reference 8 - Optimization (9 Design Variables) . . . . .	16
4	Varying Aerodynamic Paneling Schemes on Modified Wing Model of Reference 8 - Optimization . . . . .	18
5	Environmental, Initial Geometrical and Material Property Model Data .	20
6	Spanwise Structural Variation, High Aspect Ratio Wing Model Flutter Analysis (Aero Mesh 7 x 5) . . . . .	23
7	Spanwise Structural Variation, High Aspect Ratio Wing Model Optimization (Aero Mesh 7 x 5) . . . . .	24
8	Aerodynamic Mesh Variation, Medium Aspect Ratio Wing Model Flutter Analysis . . . . .	29
9	Aerodynamic Mesh Variation, Medium Aspect Ratio Wing Model Optimization (31 Design Variables) . . . . .	30
10	Use of MPCs, Medium Aspect Ratio Wing Model - Flutter Analysis . . .	32
11	Use of MPCs, Medium Aspect Ratio Wing Model - Optimization I: EPS=-0.02; II: EPS=-0.03; III: EPS=-0.05 (31 Design Variables) . . . . .	33
12	Structural-Aerodynamic Interaction, Medium Aspect Ratio Wing Model	
	a) Flutter Analysis . . . . .	38
	b) Optimization . . . . .	38

# LIST OF TABLES, Continued

Table	Page
13 Chordwise Structural Variation, Low Aspect Ratio Wing Model Flutter Analysis (Aero-Mesh 15 x 15) . . . . .	41
14 Varying Spar Number on Low Aspect Ratio Wing Model - Optimization Aero Mesh a) 5 x 5 b) 15 x 15 . . . . .	42
15 Variation of Input Mach Number, Low Aspect Ratio Wing Model Flutter Analysis (5-Spar, Aero Mesh 15 x 15) . . . . .	45
A-1 Influence of Selection of Reduced Frequency Values on Optimization Structural-Aerodynamic Interaction, Medium Aspect Ratio Wing Model	53
A-2 Influence of Selection of Various Parameters on Optimization Variation of MPCs, Medium Aspect Ratio Wing Model Shear Webs for Ribs	
a) k-Values: 0.1, 0.25, 0.5, 1.0, 2.0, 5.0, 10.0, 20.0 EPS-Values: I: -0.02; II: -0.03; III: -0.05 . . . . .	55
b) k-Values: I : 0.025, 0.05, 0.10, 0.20, 0.40, 0.80, 1.6, 3.2 II: 0.030, 0.05, 0.10, 0.30, 0.50, 1.00, 3.0, 5.0 (partial results from Table 11) . . . . .	57
c) k-Values: I : 0.02, 0.05, 0.10, 0.20, 0.50, 1.0, 2.0, 5.0 II: 0.10, 0.25, 0.50, 1.00, 2.00, 5.0, 10.0, 20.0 .	58
B-1 Varying Wing Offset from Fuselage Centerline (FCL) on Modified Low Aspect Ratio Wing Model - Flutter Analysis . . . . .	63
B-2 Varying Aerodynamic Paneling Scheme on Modified Low Aspect Ratio Wing Model - Flutter Analysis . . . . .	65



# INFLUENCE OF STRUCTURAL AND AERODYNAMIC MODELING ON FLUTTER ANALYSIS AND STRUCTURAL OPTIMIZATION

## SECTION I

### INTRODUCTION

The influences of the structural and aerodynamic modeling on flutter analysis and multidisciplinary optimization of fully built-up finite element wing models in an aeroelastic environment are not yet well understood. Therefore, the dynamic aeroelastic and optimization capabilities in the Automated STRuctural Optimization System (ASTROS) were used to evaluate the flutter behavior and structural optimization behavior with flutter constraints of various representative fully built-up finite element wing models in subsonic and supersonic flow. ASTROS was here used to calculate flutter speeds and frequencies and to minimize the weight of these wing models in subsonic and supersonic flow under given flutter and frequency constraints to determine the effect of these modeling factors.

First, the performance of the flutter module was tested against results from other codes (MSC/NASTRAN, FASTEX) on a straight and uniform wing used by Rudisill and Bhatia and various other researchers for optimization and flutter analyses. Also, the optimization module was evaluated performing optimization with a flutter constraint. Results were compared against those reported in the literature for the same wing with good agreement.

the selection of the constraint retention parameter, the reduced frequency range and actual values, and the upper frequency limit for the inclusion of modes into the flutter analysis and flutter constraint calculations; 2) Appendix B, the description of a modified low aspect ratio wing model to be used for multidisciplinary structural optimization with steady and unsteady aeroelastic constraints together; this appendix includes some discussion on the effects of the wing offset from the fuselage centerline and on aerodynamic paneling schemes; and 3) Appendix C, some thoughts on the integration of structural optimization with a nonlinear transonic flow computational environment.

## SECTION II

### INFLUENCE OF STRUCTURAL AND AERODYNAMIC MODELING ON FLUTTER ANALYSIS AND OPTIMIZATION WITH FLUTTER CONSTRAINT

In recent years, structural optimization as required and applied by the aerospace industry has expanded in scope to include such additional disciplines as static and dynamic aeroelasticity, composite materials, aeroelastic tailoring, etc. One of the more promising multidisciplinary codes presently under development is the Automated STRuctural Optimization System (ASTROS) [1-3]. This computer code combines static, dynamic, and frequency response finite element structural modules, subsonic and supersonic steady and unsteady aerodynamic modules, and an optimization module and allows for either analysis or optimized design of given aircraft configurations. Interfering surface aerodynamics are incorporated to handle the aerodynamic modeling of combinations of wings, tails, canards, fuselages, and stores. Structures are represented by finite element models, constructed from rod, membrane, shear, plate, and other elements. Static and dynamic aeroelastic capabilities include trim, lift effectiveness, aileron effectiveness, gust response, and flutter analysis.

#### 1. Introduction

As part of an ongoing effort to gain a better understanding of the optimization process with aeroelastic constraints, the flutter analysis portion of ASTROS was used for various investigations of fully built-up finite element wing models in subsonic and

supersonic flow to determine the influences of structural and aerodynamic modeling on flutter analysis as well as splining and, thus, to investigate the behavior of the analyses modules of the code. Also, the optimization portion of ASTROS was used together with the normal modes and flutter module for various investigations of the same fully built-up finite element wing models to determine the influences of structural and aerodynamic modeling on optimization with flutter constraints and, thus, to investigate the behavior of the combined flutter and optimization modules of the code. This knowledge is incidental to the understanding of the dynamic behavior of wings during the optimization process. It will also result in better initial models and, thus, a more efficient optimization cycle.

First, the performance of the flutter analysis module was evaluated against results by other methods and codes such as the large scale finite element code MSC/NASTRAN [4] and the flutter analysis code FASTEX [5]. Similar comparisons for beam-type wing models were performed by Garner and French [6] and by Pendleton, French, and Noll [7] with good results. Also, the performance of the optimization module was evaluated against results reported in the literature. For both comparisons, the straight untapered wing (Figure 1), used by Rudisill and Bhatia [8,9], McIntosh and Ashley [10], Segenreich and McIntosh [11], and others for structural optimization with flutter constraints, was chosen since it represents one of the few models where all structural, material, and environmental data are given for aeroelastic analysis and optimization with flutter constraint.

It is well known that the normal modes response depends on the structural modeling

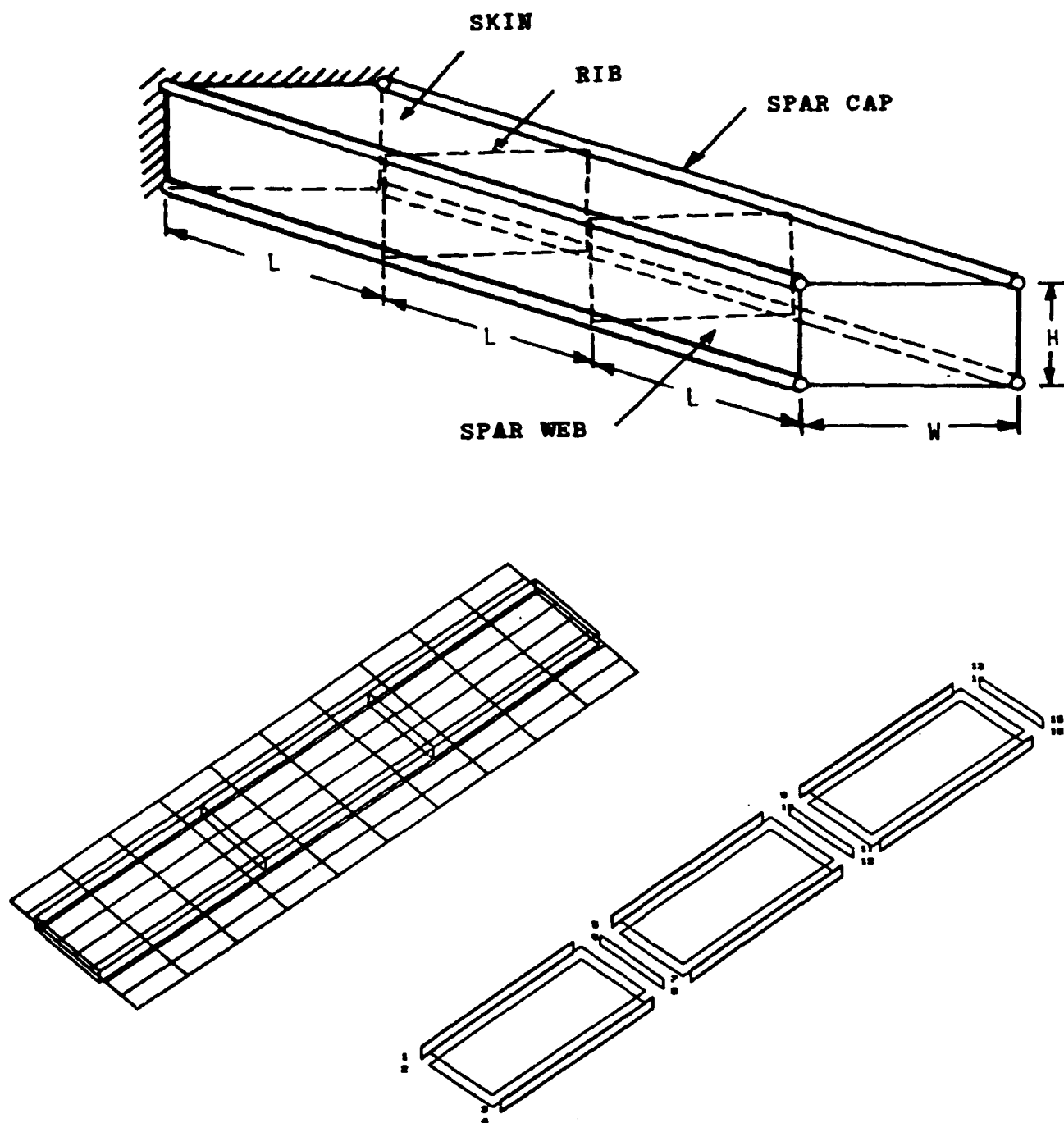


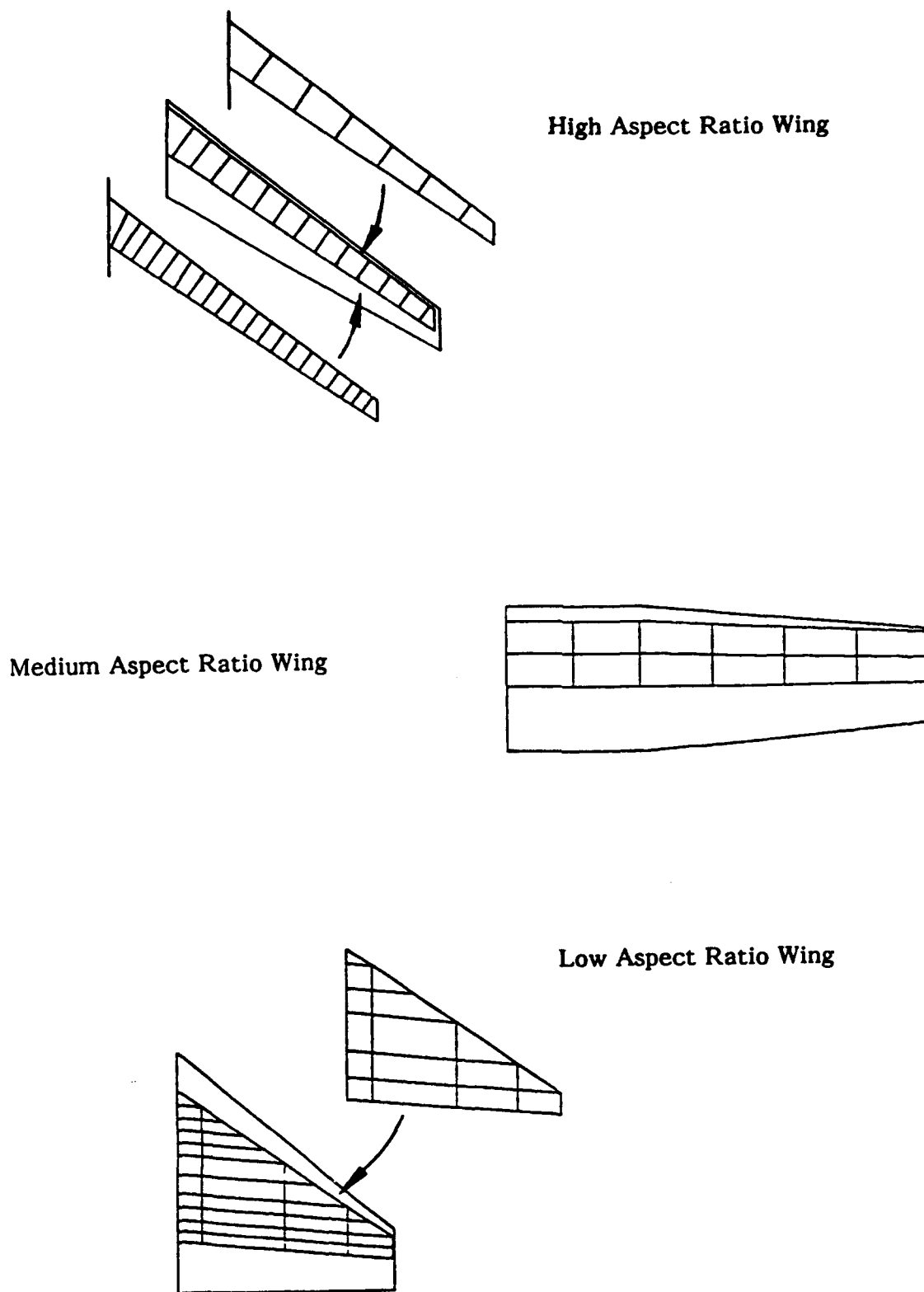
Figure 1. Wing Model of Reference 8

and the nonstructural mass distribution only, while flutter and optimization results depend on and vary with the quality of the structural and aerodynamic modeling and the splining connecting the structural and the aerodynamic representations. Thus, the main interest of this investigation was to determine the influences of the structural models, the aerodynamic models, and the splining on the free vibration frequencies and mode shapes, the flutter speeds, and the optimization behavior and minimum weights of fully built-up wings.

For this investigation, the simple rectangular unswept wing shown in Figure 1 was initially used. Then, a set of test cases was selected consisting of a high aspect ratio swept and tapered wing, a medium aspect ratio straight wing with a tapered section toward the wing tip, and a low aspect ratio swept and tapered fighter-type wing (Figure 2). The straight wing and the high aspect ratio wing were evaluated at subsonic Mach numbers while the fighter wing was investigated for flutter at subsonic and supersonic speeds. These latter three wings were modified derivatives of the wings used in the investigation of the influence of modeling on normal modes and flutter analysis by Striz and Venkayya [12] and identical to the wings investigated by the same authors in Reference 13.

## 2. Background

The following example shows the importance of this investigation: it is generally understood that membrane elements when used for spars and ribs overpredict the stiffness of a wing. Thus, when the wing used by Rudisill and Bhatia was modelled by the present



**Figure 2. Wing Models Used in the Flutter Analysis and Optimization Test Cases**

authors by replacing the front and rear spar membrane elements with shear elements, the natural frequencies of the first three bending modes dropped from 10.5, 55.9, and 125.8 Hz to 6.3, 37.6, and 110.3 Hz, respectively. This kind of change in wing bending frequencies can have a considerable impact on control surface performance and flutter. However, this example represents only a structural modeling change. In flutter analysis and optimization with aeroelastic constraints, the aerodynamic modeling also affects the results: the number, size, and distribution of the aerodynamic panels and the splining between the aerodynamic points and the structural grid. Since optimization is only as good as the associated analyses, it can, in some cases, compound and exaggerate errors arising from these. Thus, if modeling errors can have a considerable impact on the quality of the results of the associated analyses [12], optimization can be seriously jeopardized to the point where the resulting optimal design can be very unreliable. In the cited example, use of the stiffer membrane elements resulted in a 10% lower minimum weight design (38 lbs) as compared to the more realistic, less stiff shear elements (42 lbs). If flutter is the driving constraint, this could lead to the design of a structure that is potentially too weak. It is, therefore, essential that the initial designs used in optimization are feasible and modelled correctly especially when built-up finite element structural models are used rather than the previously more common beam models.

Thus, fully built-up finite element structural models for the four wings were evaluated for their flutter behavior and their performance in optimization with flutter constraint under the influence of such modeling factors as finite element selection,



structural grid refinement; number of selected modes, retention of inplane and breathing modes, selection of upper frequency bounds; aerodynamic panel size and placement; selection of reduced frequencies for aerodynamic computations; splining of the aerodynamic grid to the structural grid; selection of extra points off the structural wing box (multipoint constraint or MPCs) for better mass distribution and aerodynamic splining; solution procedures such as eigenvalue extraction routines and reduction schemes; selection of optimization parameters; etc., and results are presented.

### 3. The Rudisill and Bhatia Wing Model

The finite element wing model used by Rudisill and Bhatia and later by other researchers (shown in the exploded view portion of Figure 1) represents one of the very few cases in the flutter optimization literature where all structural, material, and environmental data were given to allow for a direct comparison of results. It was, therefore, chosen in the present study for this same purpose.

However, three drawbacks of the model have to be pointed out: a) the aspect ratio of the spar web elements in the model is 15, thus, too high for a reliable performance of the element, even in dynamic analysis; b) the spar webs are modelled by membrane elements rather than shear elements, which results in an unrealistically stiff structure; c) since no non-structural distributed mass was added to the model, the mass center of the wing coincides with the elastic axis, resulting in a close proximity of flutter speed and

divergence speed as first suggested by Eastep [14]. Here, for the base model with skins, ribs, and webs all modelled by membrane elements, the flutter speed for an input Mach number of  $M = 0.5566$  and an altitude of  $h = 10,000$  ft was calculated by ASTROS and MSC/NASTRAN as 10,881 in/sec and 10,500 in/sec, respectively, with divergence speeds of 11,900 in/sec and 11,500 in/sec, respectively. It must be pointed out that MSC/NASTRAN no longer supports pure membrane elements, but uses QUAD4 elements instead. The flutter analysis code FASTEX computed a flutter speed of 10,525 in/sec, based on the ASTROS mode-shapes, but did not show a divergence branch in the root-locus plot. The flutter speed shown in Figure 3 of Reference 8 for the initial configuration was about 10,800 in/sec. When the optimized versions of the model as obtained in References 10 and 11 were analyzed for flutter, they all encountered a divergence speed much lower than the speed used as a flutter constraint. None of these optimizations seemed to include the possibility of divergence as a flutter root with zero frequency. Thus, the size distributions of these optimized results seem to have been limited to flutter constraints only and would have resulted in designed wing models that considerably exceeded their divergence speeds.

First, to test the influence of the finite element selection on the natural frequencies, the mode shapes, and the flutter speed, the spar webs as well as the ribs were alternately modelled as shear elements and as membrane elements. The rest of the model was kept as in Reference 8. All not out-of-plane displacements were eliminated by Guyan reduction and aerodynamic MPCs were used. The results are presented in Table 1.

**Table 1. Varying Element Types on Wing Model of Reference 8**  
**Flutter Analysis**

---

<b>Ribs :</b>	<b>Membrane El.</b>	<b>Shear El.</b>	<b>Membrane El.</b>
<b>Spars:</b>	<b>Membrane El.</b>	<b>Membrane El.</b>	<b>Shear El.</b>

---

Natural	10.50 B	10.50 B	6.26 B
Freqs.[Hz]	26.60 T	26.60 T	24.75 T
	55.86 B	55.85 B	37.57 B
(Bending)	79.12 T	79.12 T	71.77 T
(Torsion)	125.83 B	125.81 B	110.35 B
	134.42 T	134.42 T	122.65 T

---

<b>Flutter</b>			
<b>Speed</b>	<b>10,881</b>	<b>10,881</b>	<b>10,400</b>
<b>[in/sec]</b>			

---

It can be seen that changing the ribs from membrane elements to shear elements did not influence the natural frequencies at all, nor did it have any impact on the flutter speed. However, when the spar webs were changed from membranes to the more realistic shear elements, there was a significant drop in the first three bending frequencies (40%, 33%, and 12%, respectively), while the first three torsion frequencies dropped by only about 8% each. The flutter speed, at the same time, dropped by about 5%, indicating that the all-membrane model was nonconservative.

Then, to examine the influence of the number of aerodynamic boxes on the wing, various paneling schemes were chosen for the model with shear elements for spar webs: 6 spanwise x 4 chordwise, 6 x 9, 15 x 4, 15 x 9, 24 x 4, and 24 x 9. Results are presented in Table 2.

Here, the results for the cases with coarse (6 x 4 and 6 x 9) spanwise mesh distribution were almost identical (0.5%) as were those of the medium (15 x 4 and 15 x 9, difference 0.5%) and fine (24 x 4 and 24 x 9, difference 0.5%) spanwise distributions. Quadrupling the spanwise distribution increased the flutter speed somewhat (4%). These results seem to indicate that a reasonably coarse mesh, used to save computer time for quick preliminary analyses, can at least result in a conservative approximation to the flutter speed.

Varying the input Mach number from  $M = 0.5566$  to 0.65 and, finally, to 0.717 for

**Table 2. Varying Aerodynamic Paneling Schemes on Modified Wing Model of Reference 8**  
**Flutter Analysis**

spanwise :	6	6	15	15	24	24
chordwise:	4	9	4	9	4	9
Flutter						
Speed	9,945	9,992	10,267	10,314	10,348	10,400
[in/sec]						

the all-membrane wing model with a 24 x 9 aerodynamic mesh, increased the flutter speed very slightly, from 10,881 in/sec to 10,943 in/sec to 11,010 in/sec, respectively. Then, a decrease in altitude from  $h = 10,000$  ft at  $M = 0.717$  to  $h = 4,500$  ft (initial conditions from Reference 11) lowered the flutter speed as expected, in this case to 10,320 in/sec.

Finally, the free vibration mode shapes computed for the base wing model showed a considerable number of inplane, breathing, and stretching modes. It was considered advantageous to eliminate these from the flutter calculations to improve convergence and to omit false flutter points which occurred when the solution algorithm jumped between modes for this case (inplane modes). From the obtained results, it became clear, however, that only the inplane modes need to be eliminated, which is most easily done by Guyan reduction to only out-of-plane displacements. Omitting those breathing and stretching modes which had mostly out-of-plane displacements in addition to the inplane modes did not seem to change the flutter results by a noticeable amount. Almost identical results were obtained with MSC/NASTRAN.

Then, the same element variations were performed to test the influence of the finite element selection on the optimization (Table 3). All in-plane displacements were again removed from the analysis set by Guyan reduction and aerodynamic MPCs were used.

Here, too, changing the ribs from membrane elements to shear elements did not have any effect on the optimization. Then, when the spar webs were again changed from

Table 3. Varying Element Types on Wing of Reference 8

Optimization (9 Design Variables)

Rib Elements:	Membrane	Shear	Membrane	Shear	Shear/Mass
Spar Elements:	Membrane	Membrane	Shear	Shear	Shear/Mass
Init. Struc. Weight:	195.92	195.92	195.92	196.04	196.04
Opt. Struc. Weight:	37.69	37.69	41.76	41.79	41.68
Aeroelastic Mode:	Divergence	Divergence	Divergence	Divergence	Divergence
	No Flutter	No Flutter	Flut. Close	Flut. Close	Flutter

membranes to shear elements, there was a significant increase in the optimum weight because the natural frequencies, especially for the bending modes, as well as the divergence and flutter speeds all dropped significantly, showing the all-membrane model to be nonconservative. When nonstructural masses were added to the all-shear model, the minimum weight stayed essentially the same, but now the divergence and flutter speeds almost coincided for the optimized structure.

Here, too, the number of aerodynamic boxes on the wing model with shear elements for spar webs was varied similar to the flutter analysis: 6 spanwise boxes x 4 chordwise boxes, 6 x 9, 15 x 4, 15 x 9, 24 x 4, and 24 x 9 were used, respectively.

The results suggest that a reasonably coarse mesh, especially in chordwise direction, can be used to save computer time for preliminary optimization and design, since it seems to result in a conservative approximation to the minimum weight (Table 4). However, for this case, results with box aspect ratios of less than 1 failed to converge.

#### 4. Three Wing Models with Different Aspect Ratios

The three wing models represent, in that order, a swept and tapered transport/bomber type wing of high aspect ratio, a straight and partially tapered light transport/combat aircraft type wing of medium aspect ratio, and a swept and tapered fighter type wing of low aspect ratio.



**Table 4. Varying Aerodynamic Paneling Schemes on Modified Wing Model of Reference 8  
Optimization**

spanwise :	6	6	15	15	24	24
chordwise:	4	9	4	9	4	9
Init. Struc. Weight:	43.3	43.5	no con-	42.5	no con-	42.3
Opt. Struc. Weight:			vergence		vergence	

As pointed out earlier, a severe deficiency in many flutter analysis reports is the absence of adequate details in the structural and aerodynamic modeling to allow for a meaningful comparison with results from other methods. Thus, for all structural and aerodynamic models used in the present investigation, all necessary dimensions and parameters are available in a report [15] to allow for such comparisons. Some selected structural and environmental data for these wings are given in Table 5.

The structural models for the three wings were built from rod, membrane, and shear elements to represent the wing boxes with spars, spar caps, spar stiffeners, ribs, and skins. Here, the rods corresponded to spar caps and spar stiffeners, the membranes were used for the skins, and the shear elements for the spar webs and the ribs of the wings.

#### a) High Aspect Ratio Wing Model

For the high aspect ratio wing, the structural weight was assumed to be 30% of the overall weight of the wing, with the other 70% distributed as nonstructural masses at all node points. No MPCs were used. For the flutter analyses and optimizations, Guyan reduction was applied to retain out-of-plane displacements only.

For this wing, the influence of structural complexity in spanwise direction was evaluated. The original wing model consisted of a reasonable box with 14 bays, showing good aspect ratios in most of the elements. Then, the wing was modelled in a simpler form with

Table 5. Environmental, Initial Geometrical and Material Property Model Data

---

**HIGH ASPECT RATIO WING:** (Transport Aircraft/Bomber,  $M = 0.87$ ,  $h = 30,000$  ft;  
 $M = 0.60$ ,  $h = 5,000$  ft)

Variation: Seven ribs, fourteen ribs, twenty-one ribs

Thick- nesses:	Shear panels:	0.145" to 0.1" in ribs (for 14-rib);
		0.2" to 0.1" in spars
	Membranes:	0.3" to 0.1" in skins

Areas:	Spar stiffeners:	0.15 in <sup>2</sup> (for 14-rib)
	Spar caps:	3.6 to 3.0 in <sup>2</sup>

---

**MEDIUM ASPECT RATIO WING:** (Light Transport/Combat Aircraft,  $M = 0.58$ ,  $h = 5,000$  ft)

Variation: No MPCs, aerodynamic MPCs (14), mass MPCs (14), all MPCs (28);  
aerodynamic mesh variations; splining

Thick- nesses:	Shear panels:	0.08" in spars/ribs
	Membranes:	0.06" in skins, 0.08" in ribs

Areas:	Spar stiffeners:	0.2 in <sup>2</sup>
	Spar Caps:	1.0 in <sup>2</sup>

---

**LOW ASPECT RATIO WING:** (Fighter,  $M = 0.85$ ,  $h = 5,000$  ft)

Variation: Five spars, ten spars; input Mach number (subsonic - supersonic)

Thick- nesses:	Shear panels:	0.08" {I} / 0.12" {II} in ribs;
		0.15 to 0.06" in spars (5-spar)
		0.135 to 0.05" le/te, 0.075 to 0.03" int., (10-spar)
	Membranes:	0.25 to 0.04" in skins

Areas:	Spar caps:	2.0 to 1.0 in <sup>2</sup> {I} / 1.0 to 0.5 in <sup>2</sup> {II} (5-spar)
		1.75 to 0.88 in <sup>2</sup> le/te, 1.0 to 0.5 in <sup>2</sup> int. (10-spar)
	Spar stiffeners:	0.05 in <sup>2</sup>

---

Material for all wings is Aluminum:  $E = 10,000,000$  lb/in<sup>2</sup>,  $\nu = 0.33$ ,  $\rho = 0.1$  lb/in<sup>3</sup>.  
All values decreasing from root to tip.

---

only 7 bays and also subdivided into a larger number of bays (21) while keeping the total weight constant. The distribution of mass and stiffness on the wing was, thus, varied without significantly changing their values. The reasonable width to length ratio of the elements was herein exceeded, especially in the seven-bay model to determine how forgiving the structural modeling process is (Figure 3). In the optimization study, a flutter constraint of 14,000 in/sec was chosen together with a lower bound of 1 Hz on the lowest natural frequency. Also, the number of design variables was varied (13 and 26).

From the results (Table 6), it seems that a spanwise increase in the complexity of the structural modeling has very little, if any, influence on the natural vibration and flutter behavior since it only accounts for a more uniform distribution of the mass and stiffness without changing their overall values. The flutter results show the expected increase as input Mach number and altitude are changed from  $M = 0.60$  at 5,000 ft to  $M = 0.87$  at 30,000 ft, but show very little differences between the three models for the same respective flight condition. These small existing differences can possibly be attributed to a slight deterioration in the quality of the aspect ratios of the panels for the 7- and the 21-bay wings from those of the 14-bay wing as well as to the way the wing root section is modelled between the three wings.

For the optimization, the most reasonable 14- bay wing showed the most conservative results (Table 7) while the other two wings yielded lower minimum weights. This could be due to the stiffness distributions in the respective models, especially in the

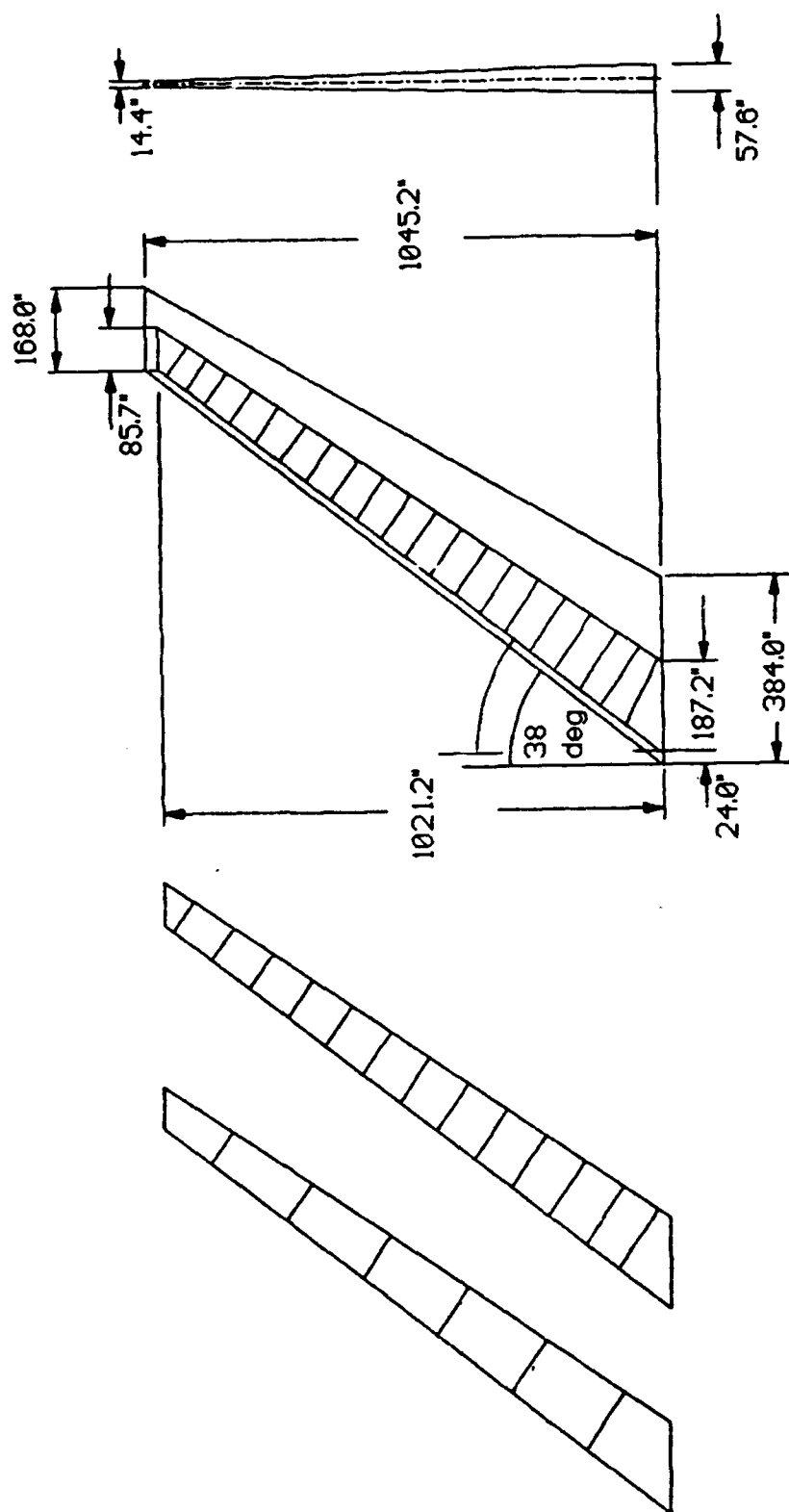


Figure 3. High Aspect Ratio Wing Model

**Table 6. Spanwise Structural Variation, High Aspect Ratio Wing Model  
Flutter Analysis (Aero Mesh 7 x 5)**

# of Ribs:	Seven	Fourteen	Twenty-One
Natural	1.09 B	1.08 B	1.09 B
Freqs.[Hz]	4.04 B/T	3.99 B/T	4.05 B/T
	8.67 T	8.74 T	8.76 T
(Bending)	9.48 T/B	9.29 T/B	9.37 T/B
(Torsion)	15.24 T/B	15.43 T/B	15.51 T/B
	16.73 T/B	16.45 T/B	16.47 T/B
Flutter [M = 0.60]	14,607	14,721	14,972
Speed			
[in/sec] [M = 0.87]	20,756	20,719	20,938

**Table 7. Spanwise Structural Variation, High Aspect Ratio Wing Model  
Optimization (Aero Mesh 7 x 5)**

# of Ribs:	Seven		Fourteen		Twenty-One	
# of Design Variables:	13	26	13	26	13	26
Init. Struct. Weight:	10206	10206	10205	10205	10205	10205
Opt. Struct. Weight:	6409	6341	6498	6448	6372	6352

root area, or due to the somewhat excessive aspect ratios in some of the elements. Comparing the V-g plots (Figures 4a,b,c) for the three models before and after the design process shows that the optimization caused the first flutter mode to approach the constraint flutter speed. Here, all three cases show almost identical results. Finally, in all cases, an increase in the number of design variables resulted in a lower weight as expected since a finer discrete distribution of masses is possible.

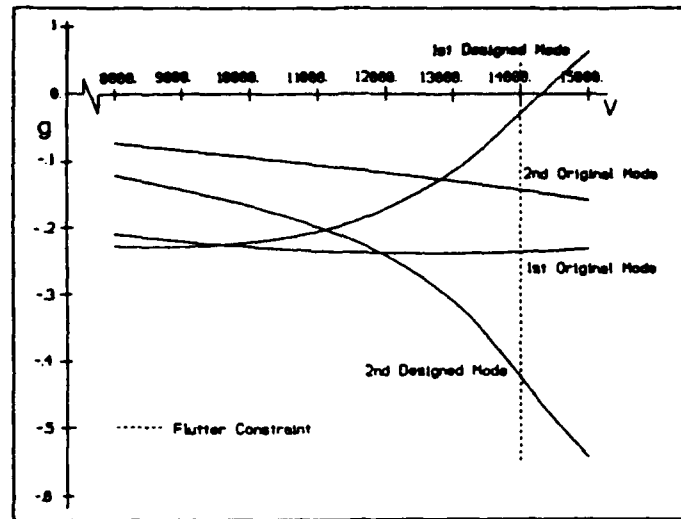
#### b) Medium Aspect Ratio Wing Model

For all models of the medium aspect ratio wing (Figure 5), the structural weight was assumed to constitute about 30% of the overall weight of the wing, with the other 70% distributed as nonstructural masses at all structural nodal points and MPCs. For the optimization, the flutter constraint chosen was 14,000 in/sec.

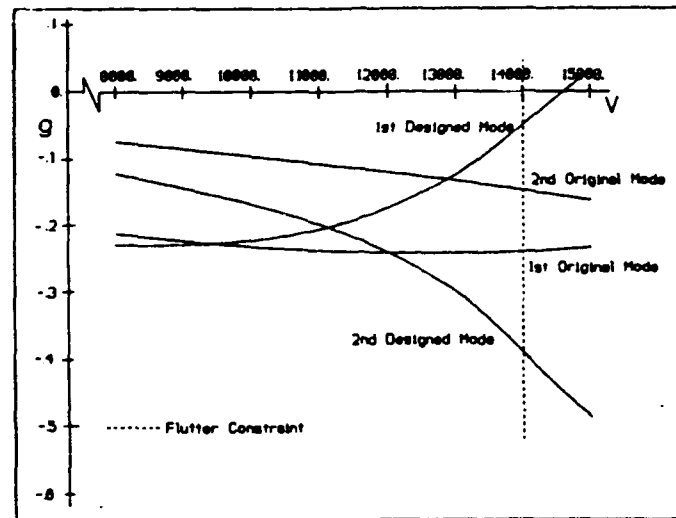
Here, the influence of the aerodynamic wing model complexity was evaluated as follows: the number of aerodynamic boxes on the wing was increased from an initially very coarse grid (5 spanwise by 5 chordwise) by increasing the number of spanwise subdivisions to 11 and 22. Then, the number of aerodynamic boxes on the wing was increased from the same coarse initial 5 x 5 grid by doubling the number of chordwise subdivisions. For most of the cases, the reasonable width to length ratio of the aerodynamic boxes was exceeded to determine how forgiving the aerodynamic modeling process is.



a) 7 Ribs



b) 14 Ribs



c) 21 Ribs

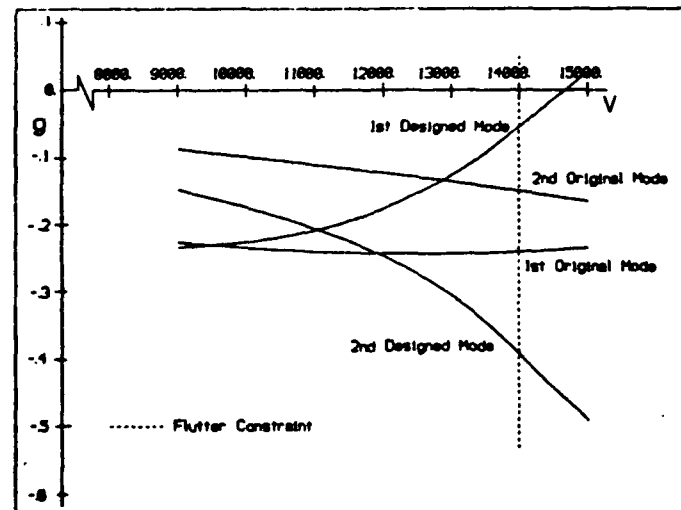


Figure 4. V-g Plots for High Aspect Ratio Wing Model: a) 7 Ribs, b) 14 Ribs, c) 21 Ribs  
26 Design Variables

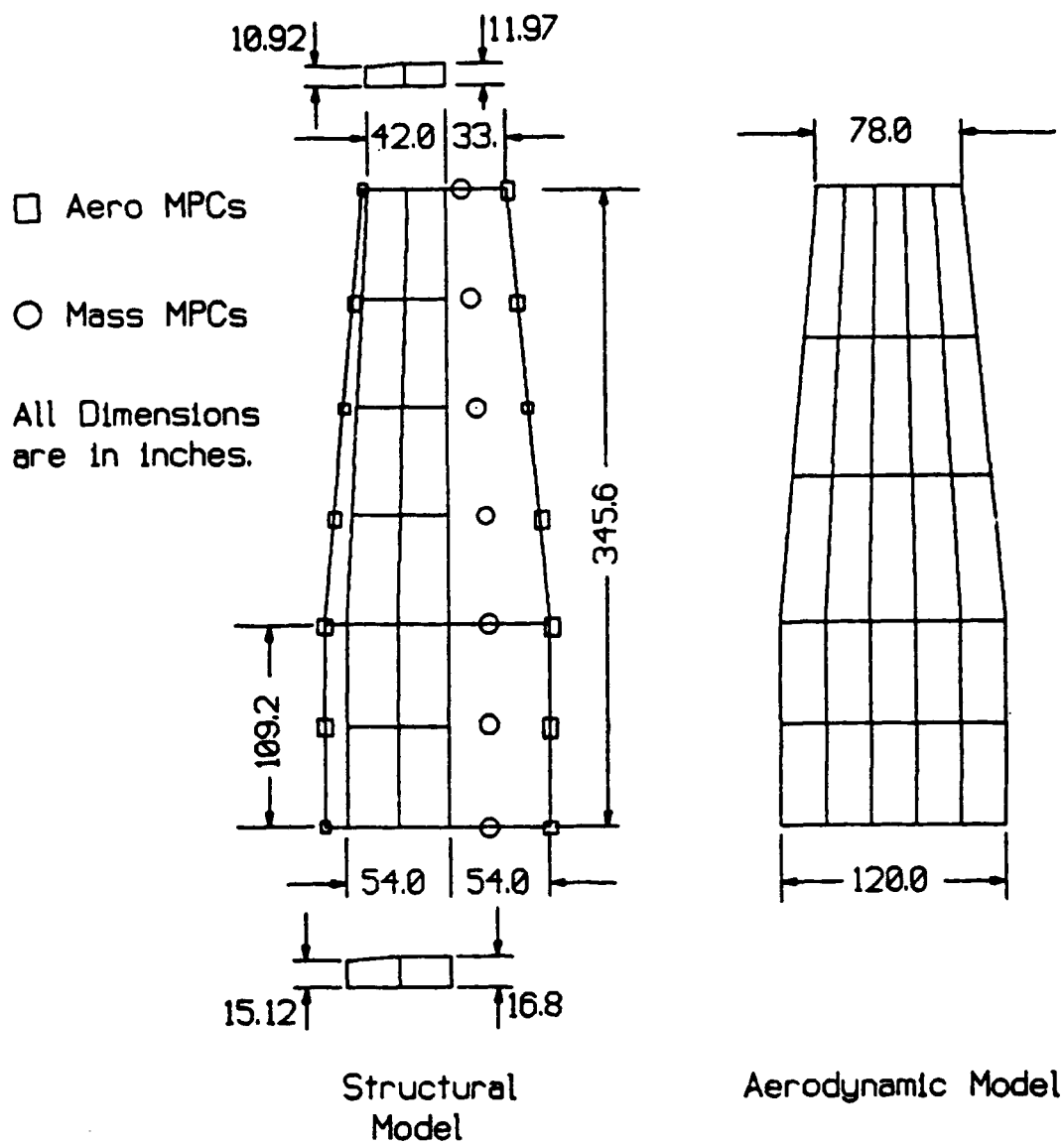


Figure 5. Medium Aspect Ratio Wing Model

The results are presented here in comparison to a more reasonable spanwise and chordwise subdivision of  $22 \times 10$  (Table 8). Similar to the results for the Rudisill and Bhatia wing model, the flutter speed changed little for all the different types of meshes. Here, as for the Rudisill and Bhatia wing, the models with a lower number of chordwise boxes showed slightly lower flutter speeds while increasing the number of spanwise boxes raised the flutter speeds.

In the optimization, the models with less spanwise boxes showed slightly higher minimum weights with virtually no variation due to a change in the number of chordwise boxes. This seems to indicate that a coarse aerodynamic mesh can be used for preliminary design and will result in a conservative design (Table 9).

Then, the use of multipoint constraints (MPCs) was evaluated. These MPCs add nonstructural points rigidly splined to existing structural points for two purposes: to attach masses for better overall mass distribution and to add points to which the aerodynamic loads can be splined for better aerodynamic load distribution (Figure 5). They had been used in all above mentioned computations for the medium aspect ratio wing. Here, the splining and the mass points were omitted on a model with an aerodynamic mesh of  $22 \times 10$ . Only out-of-plane displacements were included in the analyses.

For all cases, the main flutter mode occurred with an average flutter frequency of 7.35 Hz and with flutter speeds varying between 22,800 to 20,200 in/sec. For the cases of

Table 8. Aerodynamic Mesh Variation, Medium Aspect Ratio Wing Model  
Flutter Analysis

Panel Mesh:	5 x 5	5 x 10	11 x 5	11 x 10	22 x 5	22 x 10
Flutter Speed [in/sec]	19,512	19,581	19,912	19,969	20,167	20,240

**Table 9. Aerodynamic Mesh Variation, Medium Aspect Ratio Wing Model  
Optimization (31 Design Variables)**

Panel Mesh:	5x5	5x10	11x5	11x10	22x5	22x10
Init. Struc. Weight:				576.8		
Opt. Struc. Weight:	177.1	177.3	170.6	168.6	167.5	166.5

no and all MPCs, additional crossovers of the flutter curve were found at lower speeds (15,500 and 12,200 in/sec, respectively) and at flutter frequencies of about 16.45 Hz. These represented a slowly crossing mode and a hump mode, respectively. Finally, for the no-MPC case only, divergence was found at 24,200 in/sec. The results in Table 10 show that the use of MPCs for better distribution of the nonstructural mass away from just the structural wing box has the effect of lowering the natural frequencies slightly. Also, larger rotational moments are produced due to this offset. This effect, together with that of the MPCs used for splining the aerodynamic forces to a larger area than just the structural wing box, dropped the flutter speed for the lowest frequency flutter mode by about 12%. From the additional modes encountered with the no-MPC wing model, the use of MPCs seems desirable for a realistic flutter analysis, at least for wings which have the structural wing box located such that the elastic axis and center of mass are in close proximity.

For the optimization, Guyan reduction to only out-of-plane displacements was used, while three different values of the constraint retention parameter EPS were applied: -0.02, -0.03, and -0.05, as well as two values for the upper frequency bound on the modal flutter analyses: 50 Hz and 100 Hz. For this study, the vertical spar stiffeners were eliminated and the ribs converted from shear to membrane elements to eliminate breathing modes.

In the optimization (Table 11), for a given combination of upper frequency limit and constraint retention parameter EPS, the use of MPCs for better distribution of the non-structural mass away from just the structural wing box seems to have the effect of

Table 10. Use of MPCs, Medium Aspect Ratio Wing Model

Flutter Analysis

	Without MPCs	Aero MPCs	Mass MPCs	All MPCs
Natural	3.22 B	3.22 B	3.22 B	3.22 B
Freqs.[Hz]	16.40 B/T	16.40 B/T	16.31 B	16.31 B
	20.14 T	20.14 T	18.72 T	18.72 T
(Bending)	41.16 T	41.16 T	40.43 B/T	40.43 B/T
(Torsion)	48.35 T	48.35 T	45.01 T	45.01 T
(Breathing)	73.13 Br	73.13 Br	68.91 T	68.91 T
Flutter	15,563 (16.6 Hz) low		12,239 (16.5 Hz) hump	
Speed	22,779 (7.3 Hz)	21,395 (7.4 Hz)	21,156 (7.3 Hz)	20,238 (7.4 Hz)
[in/sec]	24,220 divergence			

Table 11. Use of MPCs, Medium Aspect Ratio Wing Model, Optimization

I: EPS=-0.02; II: EPS=-0.03; III: EPS=-0.05

(31 Design Variables)

MPCs:		None		Aero		Mass		Aero+Mass	
Up. Freq. Bounds:		50	100	50	100	50	100	50	100
[in Hz]									
Init. Struc. Weight:		576.8							
Opt. Struc. Weight:	I	170.3	184.2	157.4	157.1	229.9	477.0	175.6	180.0
	II	179.1	184.2	157.4	157.1	229.9	477.0	175.3	175.6
	III	179.1	186.4	157.4	157.1	229.9	477.0	175.6	206.4

k-values for this analysis were: 0.03, 0.05, 0.1, 0.3, 0.5, 1.0, 3.0, 5.0



increasing the optimized weight coupled with a lowering of the flutter speed found in the accompanying analysis. This may be caused by the larger rotational moments produced by these offsets. The use of MPCs for splining the aerodynamic forces to a larger area than just the structural wing box had the opposite effect, i.e., the optimized weight was even lower than for the case with no MPCs. This was consistent with an increase in the flutter speed from the accompanying analysis. When the two sets of MPCs were combined, however, the minimum weight of the structure was comparable to that for the case of no MPCs. Thus, mass MPCs seem to be a necessity for obtaining a conservative weight in optimization, even though the lack of aerodynamic MPCs may result in too high a minimum weight. The results for the optimization do not show the same common trend that was encountered in the flutter analysis, i.e., that of the common lowest frequency flutter mode, since the optimization cannot distinguish between an important mode and one of less importance (e.g., a hump mode). V-g plots of the wing with all MPCs before and after the optimization (Figure 6) show that the first designed-mode flutter speed was almost identical to the constraint flutter speed as expected while the second designed mode represented a divergence mode, which is again not unexpected for such a straight wing. Next, an increase in the upper frequency limit, i.e., in the number of modes retained in the flutter analyses, resulted in an increase in the minimum weight for all but the aerodynamic splining results while the effect of a change in the constraint retention parameter had, for most cases, little influence. However, both of these parameters have to be chosen with care (see Appendix A).

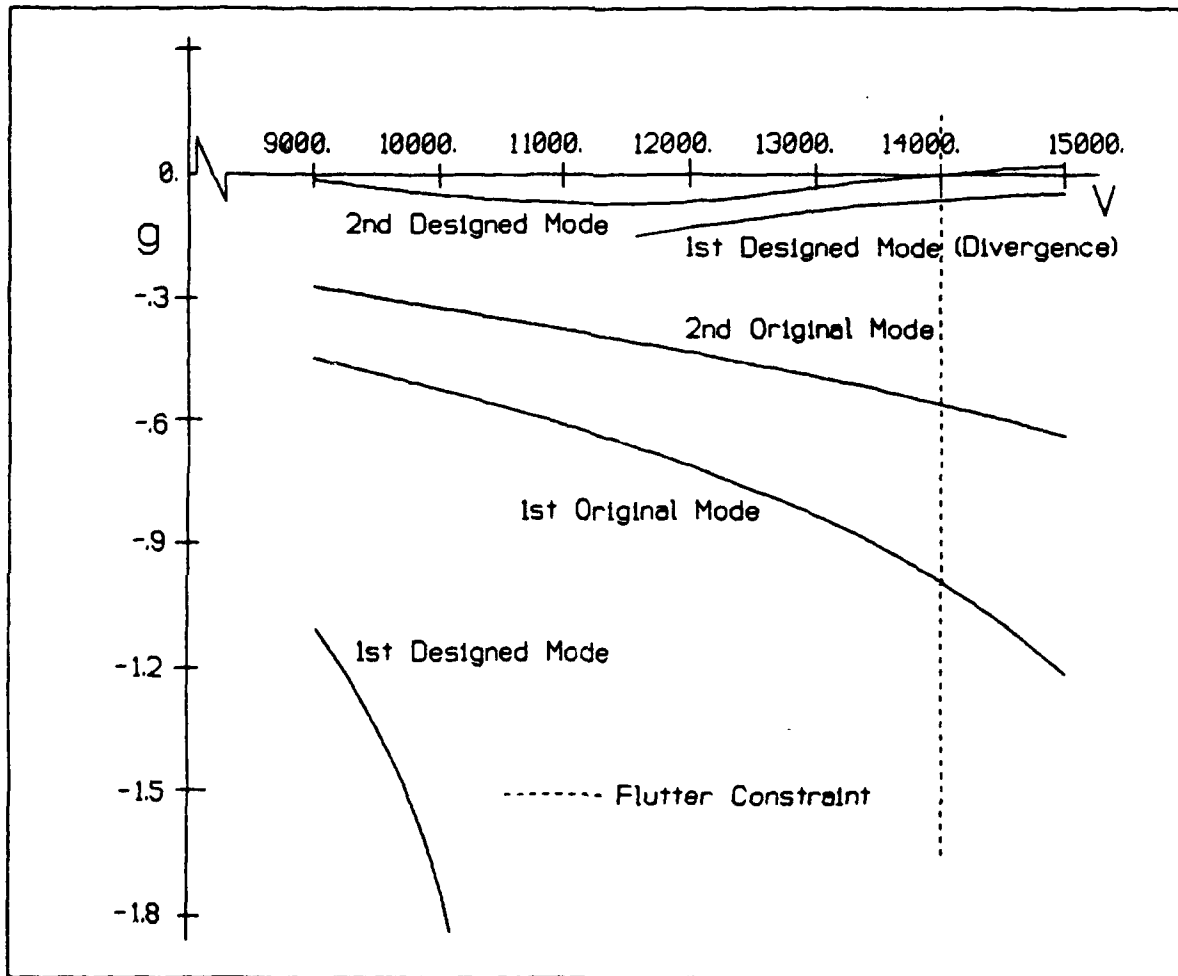


Figure 6. V-g Plot for Medium Aspect Ratio Wing Model: All MPCs, 50-Hz Upper Bound

Finally, the effects of the choice of reduced frequencies on the flutter analysis and, especially, on the optimization must be mentioned (see Appendix A). Owing to the use of cubic splines in the Mach number/reduced frequency interpolation of the aerodynamic coefficients in ASTROS, the results of the computations can show large variations for only slightly different values of reduced frequencies. In the optimization, this can result in the minimum weights converging on different local optima for two identical models with only small differences between the two sets of reduced frequencies. Thus, extreme care has to be taken in selecting the reduced frequencies. Useable optima can possibly be obtained statistically by running a number of cases with different sets of reduced frequencies and selecting an average value between the lowest weight of the lot representing the lowest weight obtainable in the optimization and the highest weight of the lot representing the most conservative design.

Finally, various overlaps were investigated for the splining of the aerodynamic coefficients to the structural grid points. The inboard (straight) and outboard (tapered) sections of the wing were treated as separate aerodynamic surfaces. All previously mentioned results were obtained with the aerodynamic coefficients for each surface splined only to the respective underlying structure. Now, the coefficients from each surface were splined to the underlying structure plus to additional rows of structural nodal points on the structure underlying the respective other surface, resulting in an overlapping splining scheme. For this study, too, membrane elements were used for the ribs instead of vertical spar stiffeners and shear webs to eliminate breathing modes.

The results (Table 12a) show a slight decrease in flutter speed as the aerodynamic forces are distributed more and more over the adjoining structural sections. As the inboard section is covered and only an increase in the distribution over the outboard section continues, the flutter speed shows a slight increase.

The optimum weights show very little variations for the different splining overlays (Table 12b) but behave consistently, i.e., with an increase in flutter speed, the optimum weight decreases, and vice versa.

#### c) Low Aspect Ratio Wing Model

For the low aspect ratio wing (Figure 7), nonstructural mass in the amount of 2400 lbs was distributed over all nodal points, and a mass of 200 lbs for a wing tip store with launcher was distributed over the wing tip points. No MPCs were used, since the wing box covers a large part of the projected wing area. An aerodynamic mesh of 15 x 15 boxes was chosen. For the optimization, an additional mesh of 5 x 5 was chosen and a flutter constraint of 25,000 in/sec was applied.

For this wing, the influence of structural complexity in chordwise direction was evaluated. Starting with a reasonable model for the wing box using five internal spars, the wing was then subdivided by adding five more spars while keeping the total weight constant. The influence of a more evenly distributed stiffness and mass arrangement was,

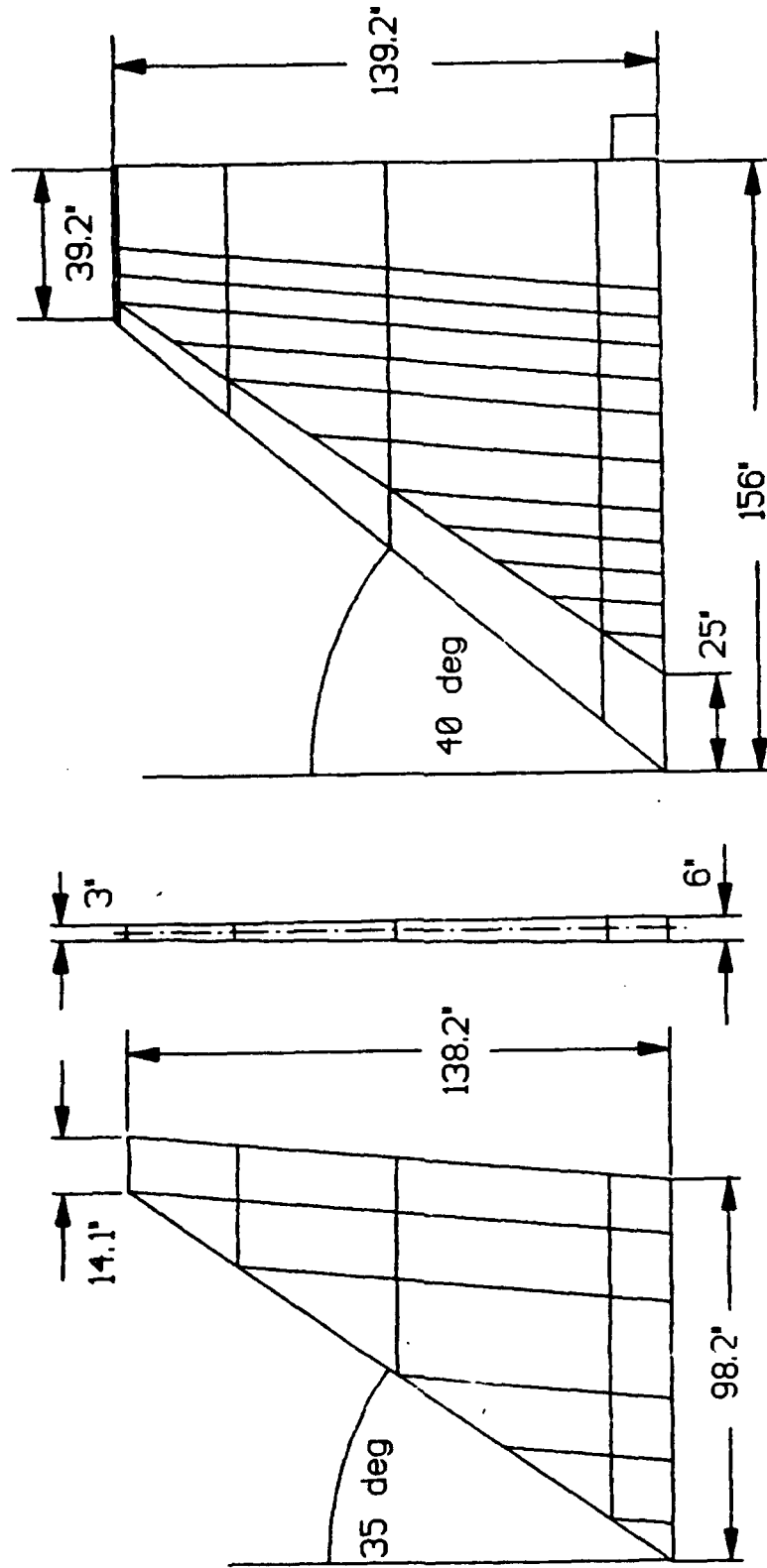


Figure 7. Low Aspect Ratio Wing Model

thus, evaluated. Results for the subsonic case with  $M = 0.85$  are presented in Table 13.

The results suggest that distributing mass and stiffness more evenly in chordwise direction reduces the natural frequencies especially in the two lowest modes while also lowering the flutter speed slightly. Thus, the coarser model in chordwise direction seems to be nonconservative.

For the optimization, results for the subsonic case ( $M = 0.85$ ) are presented in Table 14 for aerodynamic meshes of  $5 \times 5$  and  $15 \times 15$  boxes and for various numbers of design variables.

The results suggest that distributing mass and stiffness more evenly in chordwise direction allows the optimization to optimize more members and, thus, leads to lower final weights. The same is, of course, true when the number of design variables is increased. It should be noted that the 5-spar wing with 18 design variables resulted in a lower weight than the 10-spar wing with 6 design variables suggesting that it might be advantageous for the preliminary sizing of wings with flutter constraints to use a relatively simple model with a reasonably large number of design variables rather than go through the effort of creating a more complex model. Since the initial structure {I} of the 5-spar wing had somewhat oversized spar caps but undersized shear webs, both sets of values were adjusted in structure {II} to result in a 19.1% lighter wing with a more balanced size and mass distribution. However, this only resulted in a slightly lower overall weight in the

**Table 13. Chordwise Structural Variation, Low Aspect Ratio Wing Model  
Flutter Analysis (Aero-Mesh 15 x 15)**

<b>Internal Spars:</b>	<b>Five</b>	<b>Ten</b>
Natural	5.23 B	4.67 B
Freqs.[Hz]	21.18 B/T	18.29 B/T
	24.79 B/T	24.63 B/T
(Bending)	37.36 I	29.56 I
(Torsion)	37.78 B/T	37.81 B/T
(In-plane)	57.67 B/T	45.99 B/T
Flutter		
Speed	25,367	24,948
[in/sec]		

**Table 14. Varying Spar Number on Low Aspect Ratio Wing Model**

**Optimization**

**Aero Mesh a) 5 x 5 b) 15 x 15**

<hr/>					
# of Internal Spars:		Five		Ten	
# of Design Variables:		6	18	6	26
<hr/>					
Init. Struc. Weight:		I	497.8	I	497.7
		II	402.7		
Opt. Struc. Weight:		Ia	330.3	Ia	303.6
		Ib	352.6	Ib	328.5
		IIa	322.6		202.8
		IIb	362.4		208.6
			228.0		
			237.0		
			218.6		
			228.4		
<hr/>					

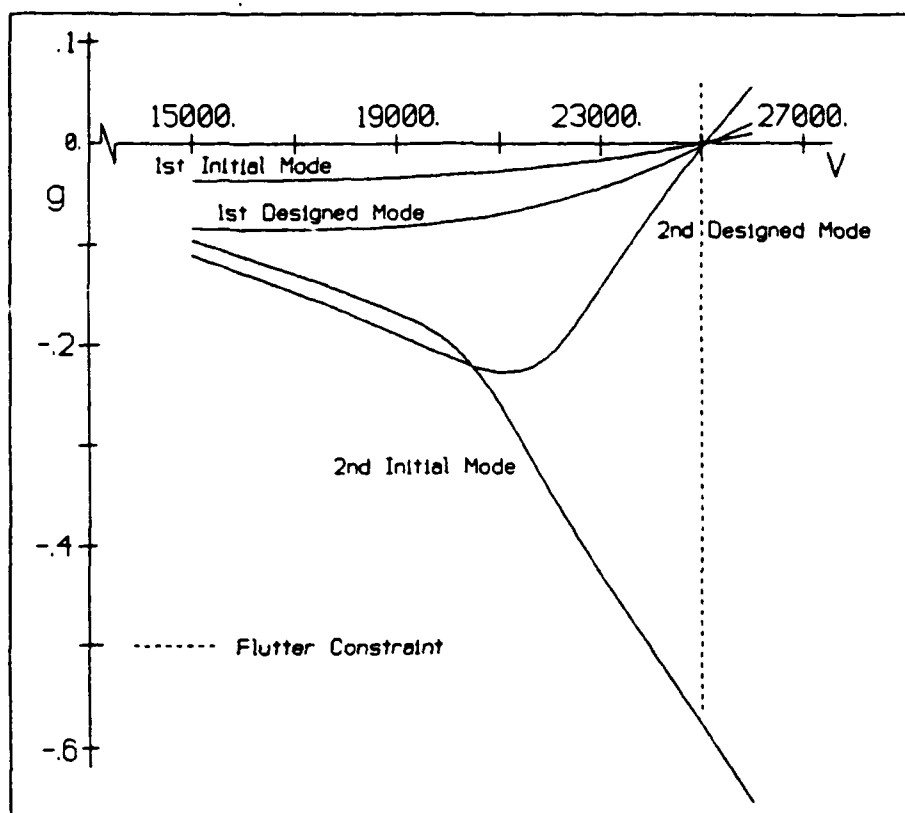


optimization (less than 5% for the structural weight and less than 0.5% for the total weight of the wing). When the fine aerodynamic mesh was chosen (15 x 15) rather than the coarse (5 x 5), the resulting minimum weights were somewhat higher (generally less than 12% for the structural weight and less than 1.5% for the total weight of the wing). However, for preliminary sizing, the coarser mesh resulted in much shorter CPU times (for 10-spar wing with 26 design variables, the CPU times were 0:12:06 for the 5 x 5 mesh and 1:28:55 for the 15 x 15 mesh on the WL/FDL VAX8650). Here, the sets of V-g plots with the first two initial and designed modes for the 5- and 10-spars wing models (Figures 8a,b) did not agree quite as well as did those for the high aspect ratio wing with spanwise distribution variation. The difference between the 5- and 10-spar models was larger in the second mode which showed a considerably larger flutter speed for the 10-spar model than for the 5-spar model. However, the trends agreed reasonably well.

Also, the influence of input Mach number on flutter speed was evaluated as the aerodynamic coefficients were calculated for subsonic ( $M = 0.5 - 0.85$ ), transonic ( $M = 0.85 - 1.2$ ), and supersonic speeds ( $M = 1.2 - 1.5$ ). It must be stressed that the aerodynamic modules in ASTROS compute aerodynamic coefficients only by linear theory and, thus, do not account for the nonlinearities of shock development in the transonic regime.

The results showed (Tables 15a and 15b) that, with an increase in input Mach number, the flutter speed decreased in the subsonic regime and increased in the supersonic

a) 5 Spars



b) 10 Spars

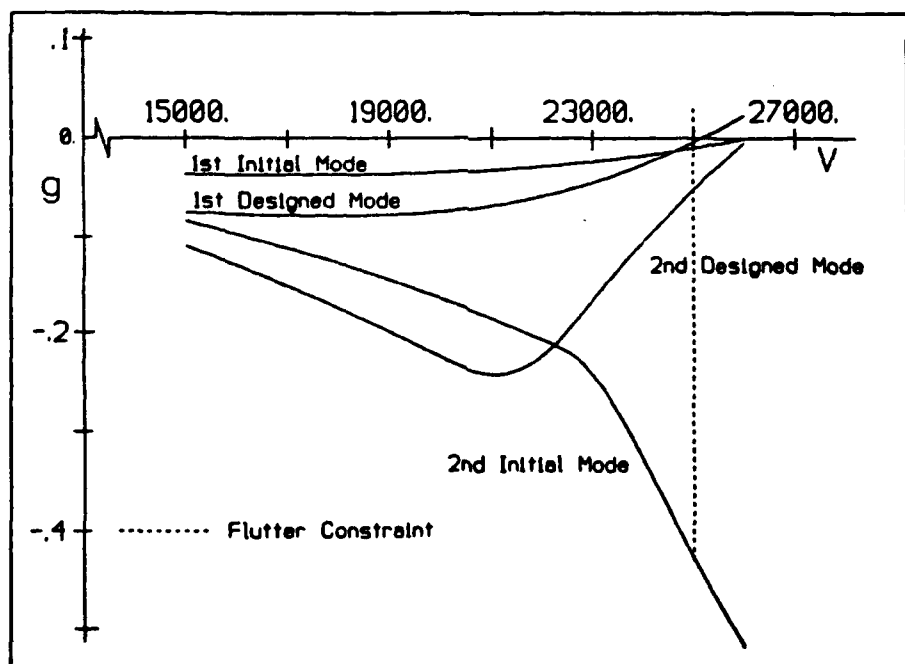


Figure 8. V-g Plots for Low Aspect Ratio Wing Model: a) 5 Spars, b) 10 Spars  
15x15 Aero Mesh

**Table 15. Variation of Input Mach Number, Low Aspect Ratio Wing Model  
Flutter Analysis (5-Spar, Aero Mesh 15 x 15)**

Initial Speed						
a) Selection [M]	0.50	0.75	0.85	0.90	0.92	0.95
- Subsonic:						
Flutter						
Speed	31,440	28,716	25,367	22,709	21,168	18,400
[in/sec]						+hump
Initial Speed						
b) Selection [M]	1.10	1.15	1.20	1.50		
- Supersonic:						
Flutter						
Speed	No Convergence	23,616	25,667	34,723		
[in/sec]		+ hump	+hump			

regime. Reasonably converged (linear) results were obtainable up to  $M = 0.92$  and above  $M = 1.2$ . At  $M = 0.95$ ,  $1.15$ , and  $1.2$ , a lower speed hump mode emerged in addition to the regular flutter mode. For  $M = 1.1$ , no converged results could be obtained. Naturally, all the results above about  $M = 0.85$  and below about  $M = 1.20$  have to be treated with extreme care since they fall in the highly nonlinear transonic regime.

## 5. Discussions and Recommendations

The influences of structural and aerodynamic modeling on flutter analysis and on optimization and the minimum weight design of built-up finite element wing models were investigated using the normal modes, flutter, and optimization modules of the Automated STRuctural Optimization System (ASTROS). This was done to gain a better understanding of the optimization process with dynamic aeroelastic, i.e., flutter constraints. Several trends could be observed during the course of the modeling, the flutter analysis, and the optimization even though it is understood that, until many more cases have been evaluated, any set of analyses has to be regarded as more or less wing type and model specific.

A quick initial evaluation of a preliminary design with a reasonably coarse grid for both the structure and the aerodynamics will result in natural frequencies and modes that are close to those from a more detailed model, while this evaluation will also result in flutter speeds and optimum weights that are, for the most part, conservative. In the flutter analysis, the chordwise distribution needs more attention than the spanwise one in the

structural modeling, while, for the aerodynamic modeling, the opposite seems indicated. In the optimization, too, a finer chordwise structural distribution seems to yield a better payoff in the form of a lower minimum weight while, for the aerodynamic modeling, a finer spanwise distribution seems preferable. In general, however, a good start is obtained for a conventional redesign process as well as for optimization.

The selection of the correct finite elements for modeling the structure is rather critical since, e.g., choosing membrane instead of shear elements for spars can result in nonconservative flutter speeds and minimum optimum weights. Further, the modes included in the optimization have to be carefully selected. In-plane modes as well as extensional modes of the vertical spar connecting rods can cause convergence problems and should be eliminated. For wings where chordwise bending modes are not expected, it is suggested to increase the frequency of the extensional modes by eliminating the connecting rods and converting the shear elements generally used for ribs to membrane elements. For fighter type wings with possible chordwise bending modes, the upper and lower wing surfaces can be connected by MPCs instead. Finally, the number of modes retained for modal flutter analysis during the course of an optimization can affect the computed optimum weights as can the selection of the constraint retention parameter. Thus, these two parameters have to be carefully chosen.

The use of mass MPCs is advised for a more realistic mass distribution, and that of aerodynamic MPCs for a better aerodynamic force distribution. However, the use of

aerodynamic MPCs can lower the minimum weights in a nonconservative fashion. Depending on the model, the omission of all MPCs can also result in increased flutter speeds and lower minimum weights and can be nonconservative as well.

Using overlaps in the splining of multiple spanwise aerodynamic surfaces seems to be mostly conservative and to have little influence on the flutter speed and the minimum weights.

Reduced frequencies sets have to be chosen with care until a more rugged interpolation scheme for the aerodynamic coefficients is incorporated in ASTROS. The constraint retention parameter, on the other hand, seems to have little influence on the optimization for most cases.

An issue of interest has resurfaced during the course of these analyses and, to some extent, the optimizations. In most cases, when a model was evaluated for flutter at subsonic speeds, a supersonic flutter speed resulted. The opposite also can occur: a subsonic flutter speed resulting from a supersonic analysis. This problem, the two-way crossing over the transonic regime, is presently being addressed in a parametric study. Initial results for a fighter wing in flutter analysis showed convergence of the (linear) aerodynamics in ASTROS up to about  $M = 0.95$  and from  $M = 1.15$  with reasonable results obtainable up to  $M = 0.92$  and from  $M = 1.2$ . As expected, the flutter speed decreased as the transonic dip was approached and increased above the transonic regime.

Future work will include investigations into the influence of how the splining of the aerodynamic forces to the structure affects the optimization, into the effect of input Mach number on optimized weight, and into the use of move limits in optimization. Optimization with strength, static aeroelastic, and flutter constraints is being performed at present to evaluate the behavior of representative wings in a true multidisciplinary optimization environment and to allow for a more general understanding of the modeling influences on such optimization.

## REFERENCES

1. Johnson, E.H., and Venkayya, V.B., "Automated Structural Optimization System (ASTROS), Vol. I: Theoretical Manual," AFWAL-TR-88-3028/I, Air Force Wright Aeronautical Laboratories, December 1988.
2. Neill, D.J., Johnson, E.H., and Herendeen, D.L., "Automated Structural Optimization System (ASTROS), Vol. II: User's Manual," AFWAL-TR-88-3028/II, Air Force Wright Aeronautical Laboratories, April 1988.
3. Johnson, E.H., and Neill, D.J., "Automated Structural Optimization System (ASTROS), Vol. III: Applications Manual," AFWAL-TR-88-3028/III, Air Force Wright Aeronautical Laboratories, December 1988.
4. Rodden, W.P., Editor, MSC/NASTRAN Handbook for Aeroelastic Analysis, The MacNeal-Schwendler Corporation, Los Angeles, California, 1987.
5. Taylor, R.F., Miller, K.L., and Brockman, R.A., "A Procedure for Flutter Analysis of FASTOP-3 Compatible Mathematical Models," AFWAL-TR-81-3063, Air Force Wright Aeronautical Laboratories, August 1981.
6. Garner, G., and French, M., "A Comparison of Supersonic Flutter Predictions for a Straight Wing," AFWAL-TM-88-176-FIBR, Air Force Wright Aeronautical Laboratories, May 1988.
7. Pendleton, E., French, M., and Noll, T., "A Comparison of Flutter Analyses for a 45° Swept Model," AIAA-87-2886, presented at the AIAA/AHS/ASEE Aircraft Design, Systems and Operations Meeting, St. Louis, Missouri, September 1987.
8. Rudisill, C.S., and Bhatia, K.G., "Optimization of Complex Structures to Satisfy Flutter Requirements," AIAA Journal, Vol. 9, No. 8, August 1971, pp. 1487-1491.
9. Rudisill, C.S., and Bhatia, K.G., "Second Derivatives of the Flutter Velocity and the Optimization of Aircraft Structures," AIAA-Journal, Vol. 10, No. 12, December 1972, pp. 1569-1572.
10. McIntosh, S.C. Jr., and Ashley, H., "On the Optimization of Discrete Structures with Aeroelastic Constraints," Computer and Structures, Vol. 8, No. 3/4, 1978, pg. 411-419.
11. Segenreich, S.A., and McIntosh, S.C., "Weight Minimization of Structures for Fixed Flutter Speed Via an Optimality Criterion," AIAA-75-0779, AIAA/ASME/SAE 16th Structures, Structural Dynamics, and Materials Conference, Denver, Colorado, May 27-29, 1975.



12. Striz, A.G., and Venkayya, V.B., "Influence of Structural and Aerodynamic Modeling on Flutter Analysis," AIAA-90-0954-CP, Proceedings, 31st AIAA/ASME/ASCE/AHS/ACS Structures, Structural Dynamics and Materials Conference, Long Beach, California, April 1990, pp. 110-118.
13. Striz, A.G., and Venkayya, V.B., "Influence of Structural and Aerodynamic Modeling on Optimization with Flutter Constraint," presented at the USAF/NASA Symposium on Recent Advances in Multidisciplinary Analysis and Optimization, San Francisco, California, September 1990.
14. Eastep, F.E., Private Communication.
15. Striz, A.G., "Realistic Structural and Aerodynamic Wing Models for Flutter Analysis and Structural Optimization," OU-AME-TR-90-110, University of Oklahoma, Norman, Oklahoma, January 1990 (updated January 1991).

## APPENDIX A

### INFLUENCE OF PARAMETER SELECTION ON STRUCTURAL OPTIMIZATION WITH FLUTTER CONSTRAINT FOR MEDIUM ASPECT RATIO WING MODEL

During the optimization study with flutter constraint of the medium aspect ratio wing, it became obvious that the choices of the reduced frequency values, of the upper frequency bound for inclusion of modes in the flutter analysis and constraint calculation, and of the constraint retention parameter, EPS, could drastically alter the encountered optima. This was especially prevalent for the cases of the variation in the splining of the aerodynamic forces to the structural nodal points and of the variation in the use of MPCs.

#### 1. VARIATION IN SPLINING

For the case where the aerodynamic forces were splined in increasingly overlapping fashion to the structural nodal points, the optimization seemed to jump between two different optima as the input values of the reduced frequency were varied slightly. Here, the constraint retention parameter was kept the same for all cases,  $EPS = -0.05$ , as was the upper bound of the frequency range for inclusion of modes in the flutter analysis,  $f = 50$  Hz.

The reduced frequency values chosen for this set of optimizations were  $k = 0.0275, 0.05, 0.1, 0.3, 0.5, 1.0, 3.0, 5.0$ . The only value varied was the lower bound of 0.0275, which was changed to 0.025 and 0.030; see results in Table A-1.

**Table A-1. Influence of Selection of Reduced Frequency Values on Optimization  
Structural-Aerodynamic Interaction, Medium Aspect Ratio Wing Model**

Rows of Splining Overlap:	None	One	Two	Three	All
Init. Struc. Weight:			576.8		
Opt. Struc. Weight for Lowest k-Value of:					
k = 0.0250	175.7	175.7	177.1	<u>181.1</u>	176.1
k = 0.0275	175.6	176.0	176.6	176.4	176.1
k = 0.0300	175.5	<u>181.1</u>	176.3	177.0	176.1

Other k-Values: 0.05, 0.1, 0.2, 0.5, 1.0, 2.0, 5.0

## 2. VARIATION IN MPCs

The above mentioned problem of convergence to different optima was much more pronounced in the investigation of the use of MPCs: i.e., no MPCs, only mass MPCs, only aerodynamic MPCs, or both sets of MPCs. Here, all three parameters were varied: the reduced frequency,  $k$ , the upper frequency bound for the modes used in flutter analysis,  $f$ , and the constraint retention parameter, EPS.

First, a set of  $k$ -values was kept constant:  $k = 0.1, 0.25, 0.5, 1.0, 2.0, 5.0, 10.0, 20.0$ . Here, EPS was varied between  $-0.02, -0.03$ , and  $-0.05$ . The values for  $f$  were 80 and 90 Hz. For this set of evaluations, vertical spar stiffeners and shear webs were used for the ribs in the structural model as opposed to just membranes as for the optimization cases shown in Table 11 and 12 of Section II.

Results are shown in Table A-2a. The foot notes indicate that, in some cases, convergence could not be achieved for the given  $k$ -values or overflow errors resulted. Thus,  $k = 0.25$  was changed to  $k = 0.2$  or  $0.3$ , respectively, to obtain convergence. Here, for the two very close upper frequency limits of 80 and 90 Hz, different optima are reached especially in the cases with no MPCs (higher weight for 90 Hz) and only mass MPCs (higher weights for 80 Hz).

To compare these results directly to ones using a different, lower  $k$ -value range

Table A-2. Influence of Selection of Various Parameters on Optimization  
Variation of MPCs, Medium Aspect Ratio Wing Model, Shear Webs for Ribs

a) k-Values: 0.1, 0.25, 0.5, 1.0, 2.0, 5.0, 10.0, 20.0  
EPS-Values: I: -0.02; II: -0.03; III: -0.05

MPCs:											
Upper Frequency Bounds: [in Hz]		None		Aero		Mass			Aero+Mass		
		80	90	80	90	80	85	90	80	90	
<hr/>											
Init. Struc. Weight:		576.8									
Opt. Struc. Weight:	I	169.7	217.3	160.2	194.8 <sup>1</sup>	357.3		242.9 <sup>3</sup>	177.7	182.9	
	II	166.2	230.5	159.2	159.2 <sup>1</sup>	318.7	273.6	189.2 <sup>1</sup>	178.3	182.9	
	III	176.6	282.3	159.2	159.0 <sup>2</sup>	318.7		194.9	178.0	182.9	
I†		304.5			158.8			204.7			183.7‡

<sup>1</sup> k = 0.20 used instead of k = 0.25

<sup>2</sup> No convergence for k = 0.25; overflow problems for k = 0.20; convergence for k = 0.30

<sup>3</sup> Overflow problems for k = 0.25; convergence for k = 0.20

† k-Values: 0.02, 0.05, 0.1, 0.2, 0.5, 1.0, 2.0, 5.0

‡ Not fully converged

( $k = 0.02, 0.05, 0.1, 0.2, 0.5, 1.0, 2.0, 5.0$ ), a single set of optimizations with  $EPS = -0.02$  and  $f = 90$  Hz was run for the different MPC cases and is also shown in Table A-2a. This set of results shows a considerably higher value for the case of no MPCs while the results for the other cases are quite comparable.

Next, various reduced frequency sets were evaluated for different upper frequency limits (25, 40, 50, 75, and 90 Hz) with  $EPS = -0.02$ . In all of these investigations, the ribs were modelled by membranes as in the original optimization studies and results for 50 Hz can, thus, be directly compared to those in Table 11 of Section II. All resulting data are shown in Tables A-2b and A-2c.

The results show, in general, little variation for different upper frequency limits, but sometimes large variations for different reduced frequency ranges and different single values within such a range. However, this effect seems to be least pronounced in the case where all MPCs are used and seems to result in the largest differences for the cases with no MPCs or mass MPCs only.

### 3. RESULTS AND DISCUSSION

The results in Tables 11 and A-2 indicate that the choice of the constraint retention parameter  $EPS$  seems to have its largest influence when a larger number of modes is included in the flutter constraint calculations, i.e., when  $f$  is larger. Otherwise, increasing

Table A-2. Influence of Selection of Various Parameters on Optimization  
Variation of MPCs, Medium Aspect Ratio Wing Model, Membranes for Ribs, EPS = -0.02

b) k-Values: I : 0.025, 0.05, 0.10, 0.20, 0.40, 0.80, 1.6, 3.2  
II: 0.030, 0.05, 0.10, 0.30, 0.50, 1.00, 3.0, 5.0 (partial results from Table 11)

MPCs: Up. Freq. Bounds: [ln Hz]	None		Aero		Mass		Aero+Mass			
	25	40	50	25	40	50	25	40	50	
Optimum	I	294.7	295.0	295.5	159.4	157.1	157.4	179.0	175.5	177.2
Structural	II			170.3			157.4	233.5	288.5	285.5
Weight	II†			272.5						229.9
	II‡			294.6						175.6

† Changed k = 0.03 to 0.020, k = 0.30 to 0.20, and k = 3.0 to 2.0

‡ Lowered range by adding k = 0.01 and dropping k = 5.0

Table A-2. Influence of Selection of Various Parameters on Optimization  
Variation of MPCs, Medium Aspect Ratio Wing Model, Membranes for Ribs, EPS = -0.02

c)	k-Values:	I :	0.02, 0.05, 0.10, 0.20, 0.50, 1.0, 2.0, 5.0									
		II:	0.10, 0.25, 0.50, 1.00, 2.00, 5.0, 10.0, 20.0									
<hr/>												
MPCs:			None		Aero		Mass		Aero+Mass			
Up. Freq. Bounds:			75	90	75	90	75	90	75	90		
[in Hz]			<hr/>									
Optimum Structural	I	295.5	174.7	157.4	157.7	228.2	265.8	175.4	175.6			
	II		296.6		157.6†		254.2†		175.8			
<hr/>												

† k = 0.20 used instead of k = 0.25



EPS from -0.02 to - 0.05 and, thus, including more constraints in the optimization at each step, does not seem to result in a large variation of the optimum weights.

The selection of the number of modes to be included in the calculation of the flutter constraint and in the flutter analysis is done by specifying an upper bound on the included frequency range. As expected and confirmed by the results in Tables 11 and A-2, this parameter can affect the optimum weight to a great extent. The initial selection of  $f$  will depend on the model to be evaluated and on the information obtained from a previous modal analysis run on the nominal model. At the least, several of the lowest-frequency bending, torsion, and mixed modes should be included, while excluding any in-plane or breathing modes.

A large amount of variation in the optimization results was due to the selection of the reduced frequency values in ASTROS. From the data presented in Tables 11, A-1, and A-2, it becomes clear that the selection of the reduced frequency range and even the selection of single numbers within such a range can have an effect on the optimum weights found in the structural optimization. Thus, the presently used cubic spline routine for the calculation of the aerodynamic coefficients based on a given Mach number and reduced frequency set seems to be sufficiently erratic to warrant replacement by either a simpler routine, such as linear interpolation, or a more sophisticated routine based on higher order function interpolations.

## APPENDIX B

### MODIFICATION OF LOW ASPECT RATIO WING MODEL FOR MULTIDISCIPLINARY OPTIMIZATION

In a parallel investigation at WL/FIBR by Eastep, interest was focused on the multidisciplinary structural weight optimized design of a fighter wing of low aspect ratio using ASTROS. The optimal redesign of a preliminary finite element model representing the wing structure was obtained with constraints imposed on strength, control reversal, and flutter using both subsonic and supersonic aerodynamic theories. It was demonstrated that the optimization capabilities of the ASTROS procedure are well suited for the preliminary structural design environment. The wing model used was a modified version of the low aspect ratio wing model described in this report.

#### 1. MODIFIED LOW ASPECT RATIO WING MODEL

In order to accommodate trim and plunge/pitch rigid body modes, the wing root was offset from and connected with MPCs to an imaginary fuselage center line and, again with MPCs, from there to the center of gravity of the modelled aircraft to allow for the use of the SUPORT command for steady aeroelastic applications. The geometric configuration for this model is shown in Figure B-1. During the model development, various offsets were evaluated and various aerodynamic paneling schemes were tested and analyzed for flutter. Also, a more realistic nonstructural mass distribution was chosen (see Reference 15 of Section II).

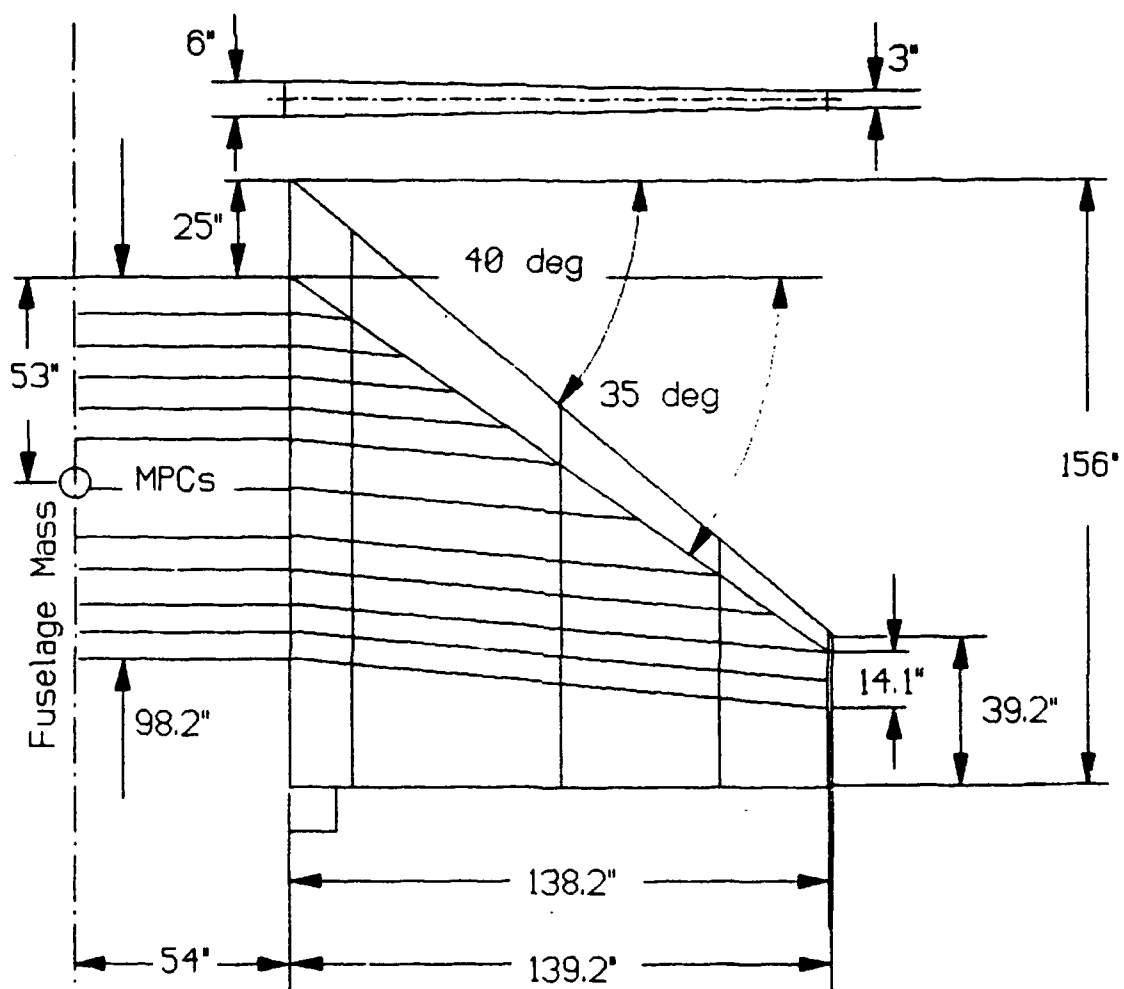


Figure B-1. Modified Low Aspect Ratio Wing Model for Multidisciplinary Optimization

## 2. OFFSET FROM FUSELAGE CENTER LINE

First, the wing was cantilevered at the root directly from the fuselage centerline with no offset. Then, the wing was investigated with offsets of 0.0, 27.0, and 54.0 inches and with MPCs to the fuselage centerline and the center of gravity. In an additional test, the wing was cantilevered directly at the root without MPCs at an offset from the centerline of 54 inches. No rigid body modes were considered for these cases. Finally, the wing with MPCs to the fuselage center line and with a 54-inch offset was evaluated with the use of the SUPORT condition for inclusion of the rigid body modes. Since numerical problems arose for this case, it was rerun with a lower range of reduced frequency values. For all these cases, one aerodynamic panel of 5 x 5 boxes was applied over only the wing. The results can be seen in Table B-1.

As expected, the results for the 0-inch offset cases with and without MPCs agreed identically as did the two cases with and without MPCs for the 54-inch offset. As the offset increased, the influence of the aerodynamic forces from the opposite wing decreased and the flutter speed increased accordingly. When the SUPORT condition was added with the original set of reduced frequencies still in force, the flutter speed dropped very slightly. It remained essentially the same, however, when the case was then rerun with a lower reduced frequency range.

Table B-1. Varying Wing Offset from Fuselage Centerline (FCL)  
on Modified Low Aspect Ratio Wing Model - Flutter Analysis

k-Values: 0.1, 0.3, 0.5, 1.0, 2.0, 5.0, 10.0, 25.0;

No SUPORT card; one aerodynamic panel on wing only

---

---

Offset:	Fixed at	MPCs to	MPCs to	MPCs to	Fixed at	MPCs to
	root, no	FCL, no	FCL, 27"	FCL, 54"	root, 54"	FCL, 54"
	offset	offset	offset	offset	offset	offset

---

Flutter

Speed	27,524	27,524	31,808	32,482	32,482	32,012 <sup>†</sup>
[in/sec]						

---

---

<sup>†</sup> with SUPORT card; some numerical difficulties encountered

### 3. AERODYNAMIC MODELING

Also, various aerodynamic paneling schemes were tested. In the last case of the wing offset investigation, one panel was applied to the wing only (5 x 5 boxes). Now, this aerodynamic panel was first extended to the fuselage centerline to account for the effects of the body in the wing root area (7 x 5 boxes), then the panel was separated into two, one on the wing (5 x 5 boxes), the other on the body section inside the wing root (2 x 5 boxes). Results are presented in Table B-2.

Here, the inclusion of the wing root to fuselage area in the calculation of the aerodynamic coefficients led to a reduction in the flutter speed since the aerodynamic forces and also the influence of the aerodynamic forces from the opposite wing increased. Finally, the creation of two separate panels raised the flutter speed by a small amount.

**Table B-2. Varying Aerodynamic Paneling Scheme  
on Modified Low Aspect Ratio Wing Model - Flutter Analysis**

k-Values: 0.03, 0.05, 0.1, 0.3, 0.5, 1.0, 3.0, 5.0;

With SUPORT card; wing connected with MPCs to FCL, 54" offset

---

Paneling:	Wing panel on wing only	One wing panel to FCL	Two wing panels, one on wing, other root to FCL
-----------	----------------------------	--------------------------	--

---

Flutter			
Speed	32,015	27,394	28,832
[in/sec]			

---

## APPENDIX C

### INCLUSION OF TRANSONIC AERODYNAMICS INTO THE OPTIMIZATION PROCESS

In the flutter analysis and the structural optimization with flutter constraint of flight vehicle structures, the region of the flight envelope most severe and least accessible computationally is the transonic regime, which can start at as low a free stream Mach number as 0.80 and reach well into the supersonic speed regime up to about  $M = 1.20$ . Here, flow nonlinearities result in moving shock waves on the dynamically moving wing structure that can, under certain conditions, lead to energy being fed into the vibration by the air stream. This, of course, could result in flutter at a lower speed than would be predicted by linear theory. Thus, a drop in the flutter speed in the transonic regime, the "transonic bucket", can be shown to exist.

Many computer codes exist that allow for the calculation of pressure distributions on flexible wings and full aircraft in transonic flow. These range in increasing order of accuracy but also program complexity from implementations of small-disturbance over full-potential to Euler and Navier-Stokes theory. Unfortunately, the better the approximation of fully nonlinear theory, the larger and more unmanageable the code. Thus, any implementation of a reasonably accurate transonic flow routine directly into a preliminary design environment would by orders of magnitude increase the computational time and



effort requirements and, thus, defeat the purpose of allowing for trade-off studies and the evaluation of many different configurations. Finally, since most transonic flow codes operate in the time domain and not in the frequency domain as do most flutter and optimization implementations, a direct interface between the aerodynamic and the structural, modal, flutter, and optimization routines would be extremely complicated.

Therefore, to credibly cover this important speed regime in a preliminary design environment such as represented by ASTROS, the nonlinear effects of transonic flow have to be incorporated into the optimization process in such a way that a reasonable trade-off exists between the efforts spent in structural optimization and the flow calculations. Discussions at WL/FIBR have led to the understanding that it is necessary to perform transonic flow calculations outside of the optimization code, i.e., to determine the effects of structural and size changes on the flow for a limited number of variables and incorporate the results into the optimization code in the form of piece-wise linear approximations. This, of course, requires that the initial models used in optimization be reasonably close to optimum designs.

In the following, an approach is presented that is expected to yield an efficient trade-off between accuracy and effort:

It is suggested that, even in the transonic regime, an initial optimization with a given flutter constraint be performed using a set of input Mach numbers in this regime but

evaluated by linear theory.

Then, since the transonic flow calculations depend on the mode shapes (normalized slopes and displacements) and natural frequencies of the structure as input, a first pass flutter analysis is performed for the same transonic Mach numbers using the transonic code with the mode shapes of the minimum weight structure which was obtained from the first optimization with linear aerodynamics. Any resulting flutter behavior (flutter frequency and mode shape) is evaluated for the influence of the first few free vibration modes, i.e., bending, torsion, mixed, and camber modes. This can possibly be accomplished through the use of FFTs or modal participation factors.

Next, an optimization is again performed with linear aerodynamics, this time with a flutter constraint chosen based on the flutter speed just calculated by the transonic code. In this optimization, the natural frequencies of the modes with largest participation in the flutter as calculated by the transonic code are modified (designed away) by using frequency constraints.

The newly determined natural frequencies and mode shapes are again incorporated into a transonic flutter analysis. The process is repeated as required.

Since sensitivities exist for the dependence of the free vibration mode shapes and frequencies (eigenvalues and eigenvectors of the eigenvalue problem) on the structural

sizes, and since the transonic aerodynamics (aerodynamic coefficients, phase shifts, and, ultimately, flutter speed) depend on exactly these same mode shapes and frequencies, the above mentioned procedure can be used to finally obtain sensitivities of the flutter speed and the aerodynamic coefficients through mode shapes and frequencies on the structural sizes that are being modified in the optimization. The use of a generalized stiffness in this context might be advantageous. These sensitivities, once computed for a range of Mach numbers and reduced frequencies, can be used in the optimization process to provide direction for modification of the structure when aerodynamics in the transonic regime are encountered.

It is recommended that reasonably efficient transonic flow codes be used for the above mentioned procedure, e.g., full-potential or small disturbance codes, rather than the prohibitively complex Euler or Navier-Stokes codes to preserve as much as possible the advantages of the preliminary design environment, i.e., speed and simplicity of computation.